Journal of Chemical Neuroanatomy 42 (2011) 72–88

Contents lists available at ScienceDirect

Journal of Chemical Neuroanatomy

journal homepage: www.elsevier.com/locate/jchemneu

The distribution of an AVT V1a receptor in the brain of a sex changing fish, *Epinephelus adscensionis*☆

Richard J. Kline [a,*], Lauren A. O'Connell [c,d], Hans A. Hofmann [c,d,e], G. Joan Holt [a], Izhar A. Khan [a,b]

[a] *Marine Science Institute, The University of Texas at Austin, Port Aransas, TX, USA*
[b] *Dexter National Fish Hatchery & Technology Center, US Fish & Wildlife Service, Dexter, NM, USA*
[c] *Institute for Cellular and Molecular Biology, The University of Texas at Austin, Austin, TX, USA*
[d] *Section of Integrative Biology, The University of Texas at Austin, Austin, TX, USA*
[e] *Institute for Neuroscience, The University of Texas at Austin, Austin, TX, USA*

ARTICLE INFO

Article history:
Received 6 February 2011
Received in revised form 15 June 2011
Accepted 15 June 2011
Available online 22 June 2011

Keywords:
Vasotocin receptor
Immunohistochemistry
In situ hybridization
Social behavior
Hermaphroditism
Rock hind

ABSTRACT

The present study describes the distribution of an arginine vasotocin (AVT) V1a receptor (AVTr) throughout the brain of a sex-changing grouper, rock hind *Epinephelus adscensionis*. The objectives of this study were to describe the AVTr distribution in the brain of rock hind for potential linkages of the AVT hormone system with sex-specific behaviors observed in this species and to examine sex-specific differences that might exist. An antibody was designed for rock hind AVTr against the deduced amino acid sequence for the third intracellular loop. Protein expression, identified with immunohistochemistry showed high concordance with mRNA expression, identified with *in situ* hybridization. AVTr protein and mRNA expression was widely distributed throughout the brain, indicating that AVT may act as a neuromodulator via this V1a receptor subtype. AVTr protein and mRNA were present in regions associated with behavior, reproduction and spatial learning, as well as sensory functions such as vision, olfaction and lateral line sensory processing. We observed high AVTr expression in granular cell formations in the internal cellular layer of olfactory bulbs, torus longitudinalis, granular layer of the corpus cerebellum, valvula of the cerebellum, nuclei of the lateral and posterior recesses, and granular eminence. High protein and mRNA expression was also observed in the preoptic area, anterior hypothalamus, and habenular nucleus. No obvious sex differences were noted in any region of the rock hind brain.

1. Introduction

Arginine vasotocin (AVT) and its mammalian homologue arginine vasopressin (AVP) influence many behavioral and physiological processes such as sexual and social behaviors, seasonal and circadian rhythms, stress response, as well as metabolic, cardiovascular and osmotic processes (see review by Balment et al., 2006). Major functions of the AVT/AVP system in the brain include control of behaviors such as social approach, courtship and aggression, with these behaviors typically attributed to males. Most notably, research with voles has revealed interspecies differences in monogamous and polygamous species attributed to differential expression of the AVP V1a receptor in specific brain regions (Insel et al., 1994; Nair and Young, 2006).

The AVP system in mammals has received the most attention, and three receptor subtypes have been identified that differ in their tissue distribution and pharmacological characterization. The three receptors, designated V1a, V1b and V2, are membrane-associated, G protein-coupled receptors that are expressed in numerous tissues throughout the body with considerable overlap (Birnbaumer, 2000). However, differences are seen in their function through second messenger systems, and major effects are discerned through pharmacological experiments. There is a clear linkage between V1a receptor expression in the brain and sex specific behaviors in mammals, birds, amphibians and fish (Baeyens and Cornett, 2006; Hasunuma et al., 2007; Insel et al., 1994; Semsar et al., 2001), while the V1b receptor mediates the vasopressor response through an action in the pituitary where it is linked with adrenocorticotropic hormone (ACTH) function (Jurkevich et al., 2005; Tanoue et al., 2004). The V2 receptor, on the other hand, regulates water uptake via aquaporins in the kidney (Hayashi et al., 1994). Both V1 receptor forms utilize the inositol phosphate second messenger system and mobilize intracellular Ca^{2+} whereas the V2 subtype is linked to the adenylate cyclase

☆ *Grant sponsor*: Bass Foundation Grant to GJH and E.J. Lund Fellowship in Marine Science to RJK.

* Corresponding author. Tel.: +1 361 749 6795; fax: +1 361 749 6749.
E-mail address: rjkline@mail.utexas.edu (R.J. Kline).

0891-0618/$ – see front matter © 2011 Elsevier B.V. All rights reserved.
doi:10.1016/j.jchemneu.2011.06.005

pathway (Birnbaumer, 2000). In mammals, the V1 type receptors can be further distinguished from one another based on differing agonist and antagonist affinities (Manning and Sawyer, 1993; Serradeil-Le Gal et al., 2002). However, similar research on specific AVT receptor agonists and antagonists is currently lacking for non-mammalian vertebrates.

Although the three major subtypes have been well characterized in mammals, the function and presence of homologous receptors are less clear in fish. Mahlmann et al. (1994) first isolated an AVT receptor in white sucker (*Catostomus commersonii*) and characterized it as pharmacologically and functionally similar to the mammalian V1a type receptor. Other investigators have shown the V1 type receptor associated with osmoregulation in the kidney is widely distributed in other fish tissues such as brain, pituitary and gill (Lema, 2010; Warne, 2001).

Recently, three forms of AVT receptor mRNA have been isolated in newt and identified by amino acid homologies and mRNA tissue distribution as V1a, V1b and V2 subtype receptors (Hasunuma et al., 2007). The two proposed V1 subtypes are highly expressed in the brain and pituitary whereas the proposed V2 subtype is highly expressed in the kidney but absent from the pituitary, similar to the distribution of the AVP system in mammals (Birnbaumer, 2000; Ostrowski et al., 1994). In pupfish (*Cyprinodon nevadensis amargosae*), Lema (2010) has isolated mRNA sequences for three AVT receptor subtypes and identified them by their mRNA tissue distribution and amino acid homologies as V1a1, V1a2 and V2 receptors. He has reported the presence of two distinct forms of the V1a subtype, with overlapping mRNA distributions in the forebrain, midbrain, cerebellum and hind brain. This study did not identify a V1b receptor in pupfish, although its existence cannot be discounted based on the data presented.

The presence of three receptor subtypes in teleost fish and their range of functions in relation to their mammalian counterparts are unclear. Numerous effects of AVT have been noted and some similar functions have been attributed to receptor subtypes as characterized in mammals, such as changes in social behavior (Semsar et al., 2001), osmoregulation (Warne et al., 2005) and smooth muscle contraction (Conklin et al., 1999). Behavior experiments in fish and amphibians have implicated a V1a type receptor based on the effects of an AVP V1a antagonist, Manning compound. With these behavioral effects attributed to the V1a receptor and the recent identification of multiple V1a type receptors by Lema (2010) with overlapping expression in the brain, there is a need for localization studies to understand receptor distribution and to infer potential function(s).

Neuroanatomical distribution of AVT binding sites has been described in only a few fish and amphibian species. In one study, fluorescently labeled AVT was administered directly to the brain of newt and specific cell populations in the reticular formation of the hind brain were labeled and identified as areas of AVT action (Lewis et al., 2005). Similarly, only one study in fish has reported identification of AVT binding sites in the pituitary and several generalized brain regions in the seabass, *Dicentrarchus labrax* (Moons et al., 1989). However, the receptor subtypes and detailed examination in specific neuronal populations could not be established using this method.

In the only published immunohistochemistry (IHC) study of an AVT receptor in fish, Warne (2001) has cloned and characterized a V1a type receptor and developed an antibody against a 15 amino acid sequence of the third intracellular loop (Warne et al., 2005). This study focused on osmoregulation in the European flounder, *Platichthys flesus* and IHC experiments with the AVTr V1a antibody revealed strong staining in kidney tissue as well as functional evidence of its role in osmoregulation. Though this study noted mRNA expression of the V1a receptor in the brain tissue, no information regarding its distribution in specific brain regions was provided.

As in mammals, sex specific behavior has been documented in several fish species and correlated with changes in AVT hormone expression in specific cell populations in the preoptic area–anterior hypothalamus (POAH). This difference has been documented in several species of sex changing fish such as wrasse, goby, and anemone fish where sex specific behavior has been correlated with AVT cell populations in the POAH that vary in relation to sexual state (Godwin et al., 2000; Grober and Sunobe, 1996; Iwata et al., 2008). The AVT V1a type receptor has been implicated in the control of certain male behaviors in different vertebrate groups because administration of an AVP V1a specific antagonist can disrupt these behaviors. The reported effects range from delayed onset of aggression and marking behavior in mammals (Albers et al., 1986; Winslow et al., 1993), reduced courtship and aggression in fish (Semsar et al., 2001) to the inhibition of clasping behavior in amphibians (Moore and Miller, 1983).

Aside from the effects of AVP V1a antagonists and sexual dimorphism of specific AVT producing cell types and a single published study on AVT binding sites listed above, little is known regarding the function and distribution of vasotocin receptors in the brain of fish. The objective of this research was to describe the distribution of an AVT receptor using an antibody designed against the deduced amino acid sequence from the AVT V1a2 receptor cDNA sequence in rock hind. In addition, the AVT V1a2 receptor mRNA expression was localized by *in situ* hybridization (ISH) to confirm specificity of the immunoreaction. Rock hind behavior and gonadal sex can be altered via manipulations of the social environment (Kline et al., 2011) and ongoing research on sex specific behaviors and AVT prompted this study on the distribution of the AVT V1a2 receptor in this species. Of particular interest are the sites of action in the brain, especially the POAH and other areas that might affect sexual behavior and have potential for downstream effects on the reproductive system.

2. Methods

2.1. Animals

Nine rock hind were captured from oil platforms in the Gulf of Mexico near Port Aransas, TX, and used immediately for IHC, ISH and Western blot studies. Sex was determined by gross examination of the gonads after the collection of brain samples. Microscopic examination showed that these fish were not in reproductive season with testis and ovaries in the early stages of development. All rock hind used in this study were treated in compliance with a protocol approved by the University of Texas at Austin Animal Care and Use Committee.

2.2. AVT receptor antiserum

Antibodies to the rock hind V1a2 subtype vasotocin receptor were raised in rabbit against a region corresponding to the predicted protein sequence (GenBank accession no. HQ141396) of the third intracellular loop of the receptor and affinity purified (Fig. 1). The two forms of the V1a receptor for rock hind differ substantially in the antigenic site of the third intracellular loop and for other vasotocin receptor forms identified in fish (Fig. 1). Although no other AVT receptor forms are available for rock hind and no V1b form has been identified in any fish, the third intracellular loop region differs substantially between V1a and V1b receptor forms in newt (Hasunuma et al., 2007).

To test the specificity of the AVTr antibody, Western blot was performed to determine which proteins were identified by the antibody. One male and one female rock hind were killed by an overdose of MS-222 (1 g l^{-1}) and whole brain removed. Brain tissue was extracted using the Q-proteome cell compartment extraction kit to isolate membrane, cytosolic and nuclear fractions (Invitrogen, USA). Membrane protein (15 μg) from each cell compartment fraction was loaded and run on a 10% sodium dodecyl sulfate–polyacrylamide electrophoresis (SDS–PAGE) gel. Following overnight transfer to polyvinylidene fluoride (PVDF) membrane, the membranes were washed 3 times for 5 min with PBS-T (20 mM phosphate base, 150 mM NaCl, 0.1% Tween-20, pH 7.6) and immersed in blocking buffer (5% normal goat serum and 0.5% porcine gelatin in PBS-T) for 1 h at room temperature. Membranes were then rinsed in PBS-T and incubated overnight at 4 °C with AVTr antibody or antibody pre-absorbed overnight with 1 μg of antigen peptide to 1 μl antibody at a final dilution of 1:1000 in PBS-T. Following primary

antibody incubation, membranes were washed 3 × 5 min with PBS-T and incubated with secondary HRP linked goat anti-rabbit antibody (AbCam, Cambridge, MA) at a final concentration of 1:5000 in PBS-T with 5% nonfat milk for 2 h at room temperature. Membranes were again washed 3 × 5 min with PBS-T, and Super-Signal West Pico chemiluminescent substrate (Pierce, Rockford, IL) was applied to visualize immuno-labeled band(s) on ECL hyperfilm (Amersham, Piscataway, NJ).

2.3. AVT receptor IHC

Three male and two female rock hind were killed with an overdose of MS-222 ($1\ g\ l^{-1}$) and a cannula was immediately introduced into the ventral aorta through which ice cold physiological saline (0.9% NaCl) with heparin ($200\ I.U.\ ml^{-1}$) was administered until the gills were pale followed by ice cold Zamboni's fixative

Table 1
Abbreviations.

AC	Anterior commissure	NLVa	Lateral nucleus of the valvula, anterior part
AON	Anterior octaval nucleus	NLVc	Lateral nucleus of the valvula, central part
AP	Accessory pretectal nucleus	NPC	Central pretectal nucleus
CCe	Corpus cerebelli	NPGc	Commissural preglomerular nucleus
CM	Corpus mamillare	NPGl	Lateral preglomerular nucleus
CP	Central posterior thalamic nucleus	NPGm	Medial preglomerular nucleus
CZ	Central zone of the optic tectum	NPOav	Anteroventral part of the parvocellular preoptic nucleus
DAO	Dorsal accessory optic nucleus	NPOpc	Parvocellular part of the parvocellular preoptic nucleus
Dc1	Central part of the dorsal telencephalon division 1	NPT	Nucleus pretectalis
Dc2	Central part of the dorsal telencephalon division 2	NRL	Nucleus of the lateral recess
Dc3	Central part of the dorsal telencephalon division 3	NRP	Nucleus of the posterior recess
Dc4	Central part of the dorsal telencephalon division 4	NSC	Suprachiasmatic nucleus
Dd	Dorsal part of the dorsal telencephalon	nSE	Nucleus subeminentialis
Dld1	Lateral zone of the dorsal telencephalon division 1	NSV	Nucleus of the saccus vasculosus
Dld2	Lateral zone of the dorsal telencephalon division 2	NT	Nucleus taenia
Dlp	Posterior division of the lateral part of the dorsal telencephalon	nIII	Nucleus of the oculomotor nerve
Dlv	Ventral division of the lateral part of the dorsal telencephalon	nIV	Trochlear nerve nucleus
Dm1	Medial part of the dorsal telencephalon, subdivision 1	nVI	Abducens nerve nucleus
Dm2	Medial part of the dorsal telencephalon, subdivision 2	OC	Optic chiasm
Dm3	Medial part of the dorsal telencephalon, subdivision 3	ON	Optic nerve
Dm4	Medial part of the dorsal telencephalon, subdivision 4	OT	Optic tectum
Dm5	Medial part of the dorsal telencephalon, subdivision 5	PCo	Posterior commissure
DMON	Decussation of the area octavolateralis	PE	Pre-eminential nucleus
DON	Descending octaval nucleus	PG	Periventricular granular cell mass of the caudal lobe
DP	Dorsal posterior thalamic nucleus	pgd	Dorsal periglomerular nucleus
Dp	Posterior part of the dorsal telencephalon	PGZ	Periventricular greay zone of the optic tectum
DT	Dorsal tegmental nucleus	Pj	Purkinje cells
DWZ	Deep white zone of the optic tectum	PLl	Perilemniscular nucleus, lateral part
E	Entopeduncular nucleus	PLm	Perilemniscular nucleus, medial part
ECL	External cellular layer of olfactory bulbs	PMgc	Gigantocellular part of the magnocellular preoptic nucleus
EG	Granular eminence	PMmc	Magnocellular preoptic nucleus
G	Granular layer of the corpus cerebelli	PMpc	Parvocellular preoptic nucleus
GL	Glomerular layer of olfactory bulbs	PPd	Dorsal periventricular pretectal nucleus
HCo	Horizontal commissure	PPv	Ventral periventricular pretectal nucleus
I	Intermediate thalamic nucleus	PS	Pineal stalk
ICL	Internal cellular layer of olfactory bulbs	PSi	Intermediate superficial pretectal nucleus
IO	Inferior olive	PT	Posterior thalamic nucleus
IP	Interpeduncular nucleus	PTN	Prethalamic nucleus
IR	Inferior nucleus of the raphe	PVO	Paraventricular organ
IV	Fourth ventricle	RI	Inferior reticular nucleus
LC	Locus coeruleus	RL	Lateral reticular nucleus
LFB	Lateral forebrain bundle	RM	Medial reticular nucleus
LT	Lateral thalamic nucleus	RS	Superior reticular nucleus
M	Molecular layer of the corpus cerebelli	S	Sensory root of the facial nerve
MAG	Magnocellular octaval nucleus	SOgs	Granular and spherical part of the secondary octaval nucleus
MLF	Medial longitudinal fascicle	SR	Superior nucleus of the raphe
MON	Medial octavolateral nucleus	SV	Saccus vasculosus
NAPv	Anterior periventricular nucleus	SWGZ	Superficial white and gray zone of the optic tectum
NAT	Anterior tuberal nucleus	T	Tangential nucleus
NC	Nucleus corticalis	TLa	Torus lateralis
NCLl	Central nucleus of the inferior lobe	TLo	Torus longitudinalis
NCW	Nucleus of the commissure of Wallenberg	TNgc	Terminal nerve ganglion cells
NDLl	Diffuse nucleus of the inferior lobe	TPp	Periventricular nucleus of the posterior tuberculum
NDLlc	Central part of the diffuse nucleus of the inferior lobe	TS	Torus semicircularis
NDLll	Lateral part of the diffuse nucleus of the inferior lobe	TTB	Tectobulbar tract
NDLlm	Medial part of the diffuse nucleus of the inferior lobe	V	Trigeminal nerve
NGa	Anterior nucleus glomerulosus	VAO	Ventral accessory optic nucleus
NGp	Posterior nucleus glomerulosus	Vc	Central nucleus of the ventral telencephalon
NGS	Secondary gustatory nucleus	VCe	Valvula of the corpus cerebelli
NGT	Tertiary gustatory nucleus	Vd	Dorsal nucleus of the ventral telencephalon
NH	Habenular nucleus	Vi	Intermediate nucleus of the ventral telencephalon
NLT	Lateral tuberal nucleus	VIII	Octaval nerve
NLTc	Lateral tuberal nucleus, central part	Vl	Lateral nucleus of the ventral telencephalon
NLTd	Lateral tuberal nucleus, dorsal part	Vm	Trigeminal motor nucleus
NLTi	Lateral tuberal nucleus, inferior part	VM	Ventromedial thalamic nucleus
NLTl	Lateral tuberal nucleus, lateral part	VOT	Ventral optic tract
NLTv	Lateral tuberal nucleus, ventral part	Vp	Postcommissural nucleus of the ventral telencephalon
NLV	Lateral nucleus of the valvula	Vs	Supracommissural nucleus of the ventral telencephalon
NP	Paracommissural nucleus	Vv	Ventral nucleus of the ventral telencephalon
nMLF	Nucleus of the medial longitudinal fascicle	Xm	Facial-vagal visceromotor column

```
                                                  +++++++++++++++
V1a2 Rock hind (AD033897) PVVILVMCYGFICHSIWNNIKYKKRKSTAGAANKNGLIGKHSVSSIT--247
V1a2 FUGU      (AY027887) PVTMLMMCYGFICHSIWKNIKFKKRKGTTGAATKNGLIGKNSVSSIT--274
V1a2 PUPFISH   (GQ981413  PVVILILCYGFICHSIWKNIKYKKKKTVAGAAGKNGLIGKCSVSSIT--248
V1a1 Rock hind (AD033901) PVAVLVFCYGLICRTIWRNLKYKTRTRRTVAEANRSGMLGRSSVSSV--275
V1a1 PUPFISH   (GQ981412) PVAVLVFCYGFICRAIWRNLKCKTRRKSADAVVEATKSGILGRSSVS--272
V1a1 FUGU      (AY027886) PVAALVFCYGFICRTIWKNLKCKTQRKSVEAVAEATGAGILGPCSVS--249
V2   PUPFISH   (GQ981414) PAVIIAICQFRIFKEIHDNLYLKSERTIAQVKKQQQQQQQTSRKNSD--261
V2   Medaka    (BAJ04637) PALIITICQIRIFREIHNNIYLKSERTVMAEVKKSDILLRFHGFKKE--295
```

Fig. 1. Amino acid sequence alignment for the third intracellular loop region of the V1a2 receptor compared with other vasotocin receptor forms in rock hind and other fish demonstrating the specificity of the antigenic site (labeled with "+") for the V1a2 receptor subtype. GenBank accession numbers are listed in parentheses.

(4% paraformaldehyde in PBS, 146 mM NaCl, 0.84 mM Na_2HPO_4, and 0.16 mM NaH_2PO_4 containing 15% saturated picric acid, pH 7.4) to fix the brain *in situ*. Rock hind were then decapitated and brains removed and stored overnight in Zamboni's fixative. The following day, brains were rinsed in 1× PBS and cryoprotected in 30% sucrose in 1× PBS overnight at 4 °C prior to embedding in OCT and storage at −80 °C. Brains were transverse sectioned on a cryostat at 20 μm and thaw-mounted onto Super-Frost Plus slides (Erie Scientific Co., Portsmouth, NH) and stored at −80 °C. Prior to use in the IHC protocol, sections were removed from −80 °C and stored in a vacuum desiccator for 30 min to equilibrate to room temperature and remove condensation. Sections were then rehydrated in 1× PBS for 15 min then incubated in 1% hydrogen peroxide in PBS for 10 min. After washing 3× in PBS, antigen retrieval was performed by incubating the slides in a Coplin jar with citrate buffer (10 mM citric acid, pH 6.0) in a boiling water bath for 15 min. After cooling for 30 min, slides were rinsed in 3× PBS, and incubated for 1 h in blocking solution (3% normal goat serum and 0.3% triton X-100 in PBS). Blocking solution was removed and sections were incubated with AVTr antibody (1:1000) in PBS at 4 °C overnight in a humidity chamber (Immuno Stain Moisture Chamber, Evergreen Scientific, Los Angeles, CA). After incubation, sections were rinsed 3× over 45 min in PBS. Sections were then incubated for 2 h with biotinylated goat anti-rabbit secondary antibody (1:200) (Vector Laboratories) in blocking solution, rinsed 3× in PBS and, incubated for 30 min with ABC reagent according to the manufacturer's instructions (Vector Laboratories, USA). Immunoreactivity was detected using diaminobenzidine (DAB) substrate (Impact DAB, Vector Laboratories, USA). Sections were dehydrated with an alcohol series followed by xylene and cover-slipped with Cytoseal 60 (Richard-Allan, Kalamazoo, MI).

2.4. IHC controls

The AVTr IHC controls included: (1) omission of primary antibody, (2) omission of secondary antibody from the protocol and (3) pre-absorption of the antibody with 1 μg of blocking peptide to 1 μl antibody diluted (1:1000) overnight at 4 °C prior to use in IHC experiments.

2.5. AVT receptor ISH

As an additional test of the specificity of the AVT V1a2 antibody, *in situ* hybridization was performed on brain sections from one male and one female rock hind and results compared. Fish were killed with an overdose of MS-222. Brains were removed and embedded in O.C.T. (Optimal Cutting Temperature Compound, Tissue-Tek, Torrance, CA) on dry ice, then stored at −80 °C. Brains were cryostat sectioned at 20 μm and thaw-mounted on Super-Frost Plus slides (Erie Scientific Co., Portsmouth, NH) and stored at −80 °C. Sections were fixed for *in situ* hybridization following the methods of Munchrath and Hofmann (2010). Probe for the rock hind V1a2 receptor (GenBank # HQ141396) was designed to exclude regions of high similarity with the V1a1 receptor (GenBank # HQ662334) and isotocin receptors from other fish species. Template for the riboprobe was 145 bp in length using the primers: FW: 5′-GACAGCAGTCTCCGCAGAAC-3′, RV: 5′-TAAACAGAGTTGCCTGGCTG-3′. Riboprobes were reversed transcribed with T7/SP6 Maxiscript in vitro transcription kit (Invitrogen) using fluorescein labeled UTP (Roche, Indianapolis, IN).

On the day of processing, slides were removed from −80 °C and allowed to equilibrate to room temperature in a vacuum desiccator. Sections were processed for nonfluorescent, non-radioactive detection of mRNA with *in situ* hybridization as described in Munchrath and Hofmann (2010). Briefly, slides were incubated in hybridization buffer (50% formamide, 5× SSC, 5× Denhardt's solution, 125 mg/ml Baker's yeast tRNA, 250 mg/ml denatured herring sperm DNA) for 2 h at 60 °C and then incubated with riboprobe overnight at the same temperature. Experimental slides were exposed overnight to sense or antisense fluorescein-labeled probes. Additional control slides were treated with RNase before hybridization with antisense probe. The next day, slides were treated with RNase A at 37 °C for 1 h followed by a decreasing series of SSC with 150 nM NaCl and 100 mM Tris (pH 7.5) at room temperature then incubated in 1:1000 anti-fluorescein-alkaline phosphatase Fab fragments (Roche) in 0.5% PBS-T for 2 h at room temperature. Slides were washed in 100 mM Tris (pH 7.5), then mRNA expression was visualized via chromagenic product with BM Purple (Roche) following manufacturer's instructions. Slides were washed and then dehydrated with an alcohol series followed by xylene and cover-slipped with Cytoseal 60 (Richard-Allan, Kalamazoo, MI).

2.6. Brain distribution and photomicrographs

Illustrations of V1a2 receptor protein expression in rock hind brain were generated using the most symmetrical sections from one male rock hind brain with expression confirmed in remaining brain sections. Sections were photographed on a Nikon Eclipse microscope with a black and white camera (Photometrics Coolsnap cf Mono). Images were imported into Adobe Photoshop (CS-2, Adobe Systems Incorporated, San Jose, CA) and a complete image of each section was created by merging 20–50 images. Outlines of sections were created using Adobe Illustrator Live Trace (CS-2, Adobe Systems Incorporated, San Jose, CA). The terminology from the three parts series on cytoarchitectonic studies of the seabass, *Dicentrarchus labrax* (Cerdà-Reverter et al., 2008, 2001a,b) was employed as the main guide for identifying and labeling regions with supplemental information from Northcutt and Davis (1983), zebrafish brain atlas (Wullimann et al., 1996) and distribution of steroid receptors in African cichlid (Munchrath and Hofmann, 2010).

Cells labeled by the AVTr antibody in immunohistochemistry experiments were categorized by shape and size. The presence of AVTr signal was identified by the presence of darkly stained cells from the DAB reaction and was confirmed on multiple individuals. Relative expression between regions was not quantified but representative intensity was hand drawn as dots corresponding to three size categories. Representative photomicrographs were taken with the microscope and camera listed above and photomerged in Adobe Photoshop. Regions of high signal were identified and labeled.

During removal of the rock hind brain, the pituitary would detach and remain in the brain case. Therefore, the pituitary was processed separately.

2.7. High magnification photomicrographs for protein and mRNA distribution

For comparison of mRNA and protein expression of V1a2 receptor, sections were photographed on a Nikon Eclipse microscope with a color camera (Photometrics Coolsnap PRO color). Images were compiled and brightness and contrast adjusted in Adobe Photoshop CS-2.

3. Results

3.1. Gross morphology

The olfactory bulbs of the rock hind are relatively small with a narrow connection to the telencephalon. The rock hind has a relatively large telencephalon as compared to zebrafish (Wullimann et al., 1996) and European seabass (Cerdà-Reverter et al., 2001a), with five lobes visible on each hemisphere (Fig. 2). In transverse sections, an extra layer adjacent to the dorsolateral part of the dorsal telencephalon was observed and is designated Dld2. The rock hind has a large optic tectum and a large cerebellum that encroaches upon the lobes of the optic tectum (Fig. 2).

3.2. Antibody characterization

Western blot analysis carried out using the rock hind AVT V1a2 antibody confirmed the presence of a predicted size band of ~45 kDa in the membrane fraction, but not in the cytosolic or nuclear fractions (Fig. 3A). No differences were observed between male and female samples (female not shown) in Western blot. Pre-absorption of the antibody prior to application in Western blot analysis prevented the appearance of any band in the membrane fraction (Fig. 3B). In transverse sections, DAB staining in AVTr immuno-positive cells was very dark brown compared to the background staining (Fig. 3C). Omission of primary antibody or secondary antibody (not shown) from the protocol as well as pre-

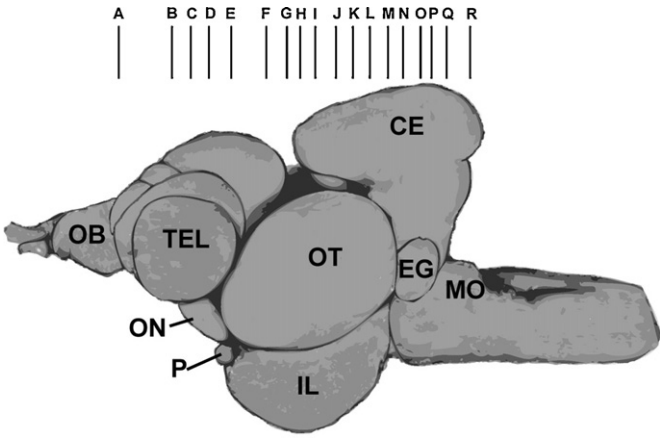

Fig. 2. Lateral view of rock hind brain with lettered lines denoting the position of transverse sections in Fig. 4. OB, olfactory bulb; TEL, telencephalon; ON, optic nerve; P, pituitary; OT, optic tectum; IL, inferior lobe of the hypothalamus; CE, corpus cerebelli; EG, granular eminence; MO, medulla oblongata. Scale bar = 1 mm.

absorption of the antibody with the peptide antigen (Fig. 3D) did not produce significant DAB staining indicating the specificity of the reaction.

3.3. ISH controls

Control slides for the *in situ* hybridization of V1a2 receptor mRNA that included pretreatment with RNAse A or incubation with the sense riboprobe showed no specific signal as compared to sections incubated with the antisense riboprobe. Close examination of antisense vs. sense treatments in the granular cell formations of the corpus cerebellum (CCe), periventricular gray zone of the optic tectum (PGZ), and torus longitudinalis (TLo) clearly showed that signal was present in these regions that was not present in the control slides.

3.4. Distribution of AVTr protein and mRNA in rock hind brain

The abbreviations used in this study are shown in Table 1. A lateral view of the rock hind brain showing gross morphological structures is presented in Fig. 2 with lines indicating locations of the transverse sections illustrated in Fig. 4. AVTr expression was high in the rock hind brain and was seen in all major regions including the olfactory bulbs, telencephalon, preoptic area, hypothalamus, posterior tuberculum, synencephalon, mesencephalon, and rhombencephalon.

The distribution of AVT V1a2 mRNA and protein in the brain of rock hind, along with photomicrographs of representative brain areas is depicted in Figs. 5–9. We did not observe any brain regions that had mRNA but not protein; therefore, we concluded that protein and mRNA distributions show high concordance. For each representative section in Figs. 5–9 a low magnification image of protein expression and nomenclature is displayed on the left side while higher magnification color images for protein and mRNA expression are shown on the right.

3.5. Olfactory bulbs and telencephalon

In the olfactory bulbs (Fig. 4A), we observed AVTr protein and mRNA expression in a dense population of small cells in the inner cell layer (Fig. 5A–C) with signal present in only few larger cells in the glomerular layer. Expression of both protein and mRNA was seen also in the large terminal nerve ganglion cells located at the medial margin of the olfactory bulbs (Fig. 4A).

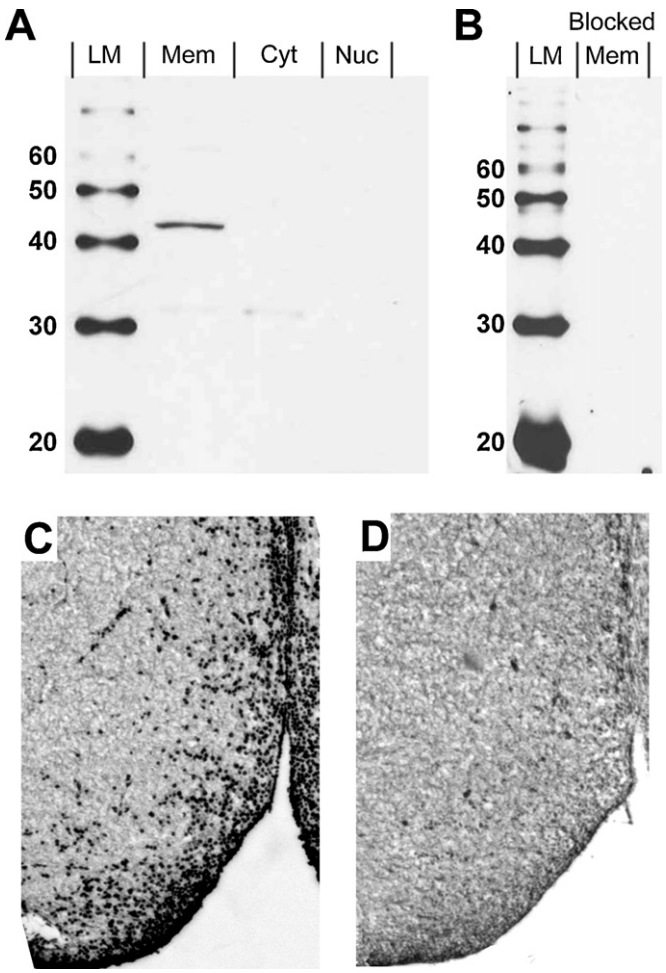

Fig. 3. (A) Western blot of rock hind brain tissue compartments labeled with the AVT V1a receptor antibody showing a prominent band of the predicted size (45 kDa) as estimated with a lane marker (LM) in the membrane fraction (Mem) but not in the cytosolic (Cyt) or nuclear (Nuc) fraction. (B) Western blot of rock hind brain membrane fraction incubated with the AVT V1a receptor antibody blocked with antigenic peptide showing the absence of any band. Transverse sections of rock hind ventral telencephalon at the level of Fig. 4E (C) showing cells labeled by the AVT V1a2 (1:1000) and secondary HRP-conjugated (1:200) antibodies, and visualized with DAB; and (D) AVTr antibody pre-absorbed with 1 $\mu g\, l^{-1}$ synthetic peptide that the antibody was raised against showing the absence of specific signal.

In the ventral telencephalon, there was a very dense expression of the protein and mRNA in the entopeduncular nucleus (Fig. 4D) and a structure resembling the lateral septal organ of birds (Figs. 4B and 5D). The dorsal nucleus of the ventral telencephalon (Figs. 4B, C and 5D), intermediate nucleus (Figs. 4D, E and 5D), and ventral nucleus (Figs. 4D, E and 5D) had many small round cells that were AVTr-positive for protein and mRNA with the highest expression occurring along the ventricular wall. The central nucleus of the ventral telencephalon had dense AVTr-positive cells in a cluster for protein (Figs. 4B and 5D) and mRNA. The supracommissural nucleus of the ventral telencephalon (Fig. 4C), the postcommissural nucleus of the ventral telencephalon (Fig. 4D), and the lateral nucleus of the ventral telencephalon (Figs. 4B, C and 5D) had many scattered small cells that were AVTr-positive for protein and mRNA.

All Dm regions had protein and mRNA expression in small round cells, with the highest expression in subdivision 2 (Fig. 4A–C) and subdivision 5 (Figs. 4B–E and 5D–F). The dorsolateral part of the dorsal telencephalon had two distinct regions: the outer margin, subdivision 1 was characterized by many small round cells expressing AVTr protein and mRNA (Figs. 4A–D and 5G, I, K) and a previously undescribed, inner division 2 (Dld2) had many medium

sized AVTr-positive cells (Figs. 4B–D and 5G). All divisions of the lateral part of the dorsal telencephalon: posterior (Fig. 4D), ventral division (Fig. 4B–D) and lateral part of the dorsal telencephalon (Figs. 4B, C and 5G) had many small round cells expressing AVTr protein and mRNA. We also observed high protein expression in small round cells of the nucleus taenia (Figs. 4B–D and 5D, F) that was confirmed with mRNA expression.

In the four major divisions of the central part of the dorsal telencephalon identified in rock hind brain expression of both protein and mRNA was observed. Dc1 had few small round cells expressing AVTr protein and mRNA (Figs. 4A–C and 5G), whereas Dc2 (Fig. 5H and J) and Dc3 had many medium sized, bipolar cells (Figs. 4B–D and 5G) and Dc4 had only few medium bipolar cells (Fig. 4C–D) that were AVTr-positive. In the posterior part of the dorsal telencephalon AVTr expression was observed in only small round cells (Fig. 4E and F).

3.6. Preoptic area and hypothalamus

In the preoptic area, we observed densely packed small cells expressing AVTr protein and mRNA in the anteroventral part of the parvocellular preoptic nucleus arranged tightly around the

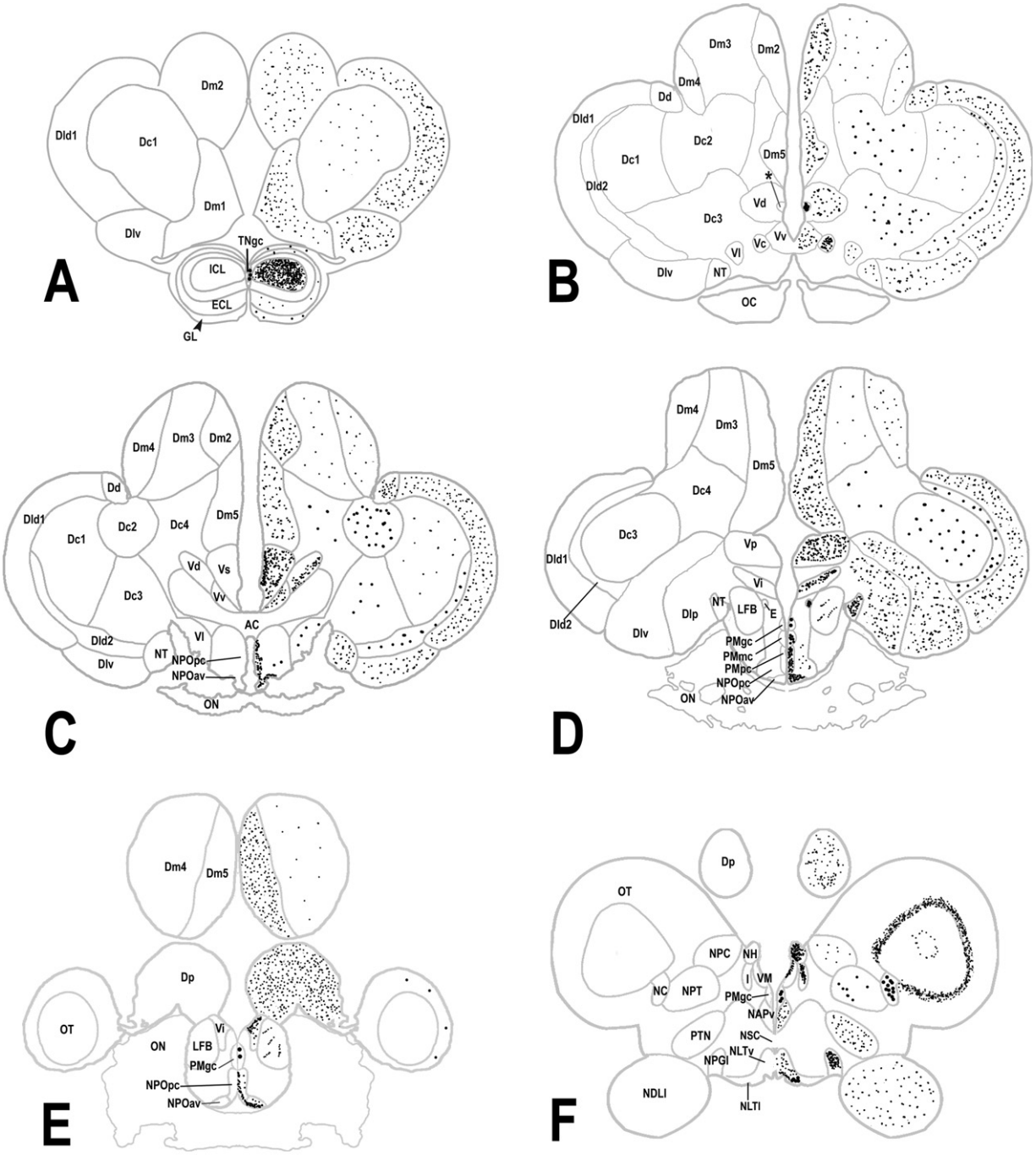

Fig. 4. (A–R) Diagrammatic representation of AVT V1a receptor expression by the brain region, and relative cell size (small, medium and large dots) and signal intensity as seen in transverse sections of rock hind brain passing through the regions indicated in Fig. 1. For abbreviations, see Table 1. The "*" indicates a region similar to the lateral septal organ seen in birds. Scale bar = 2 mm.

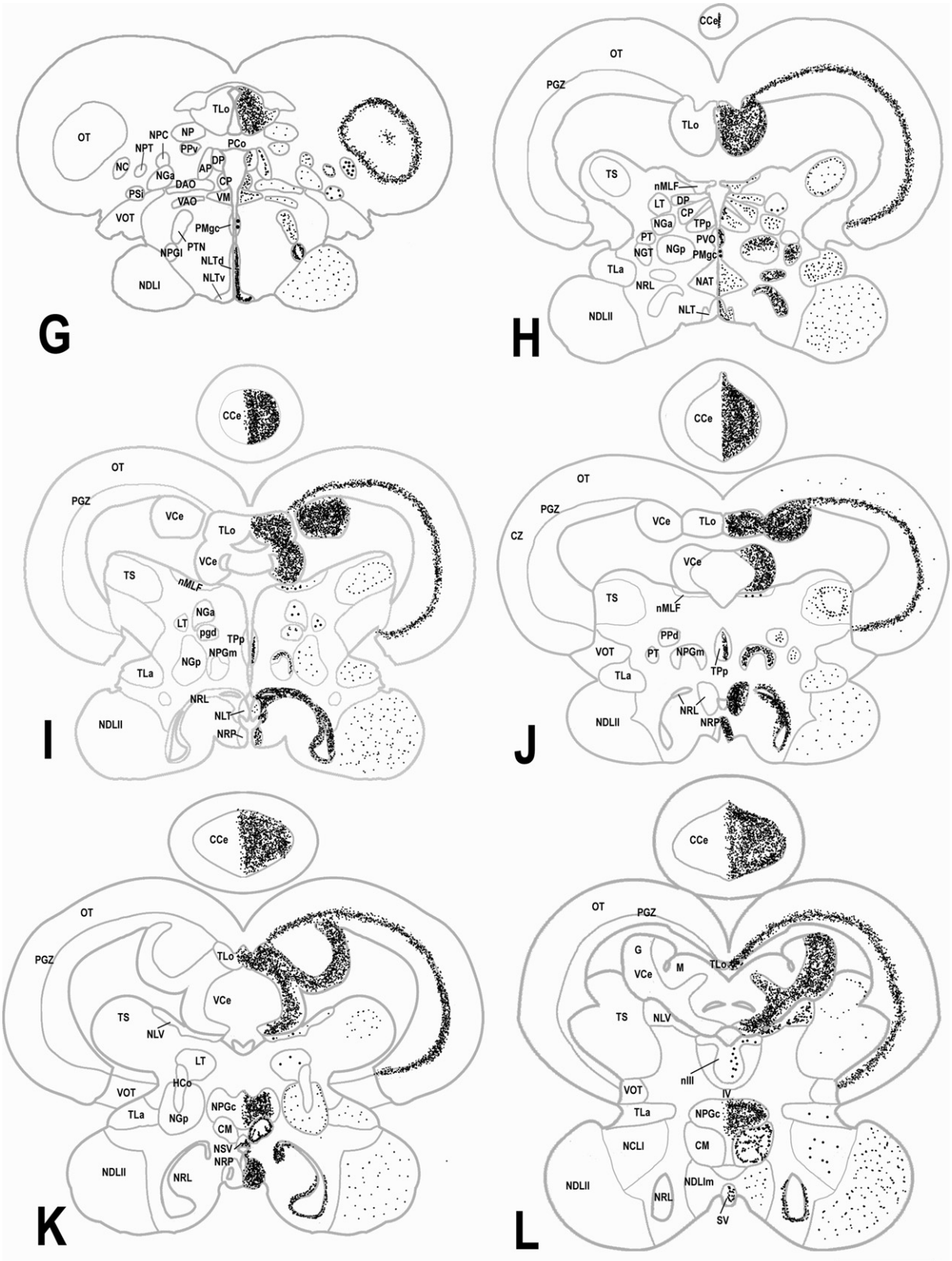

Fig. 4. (*Continued*).

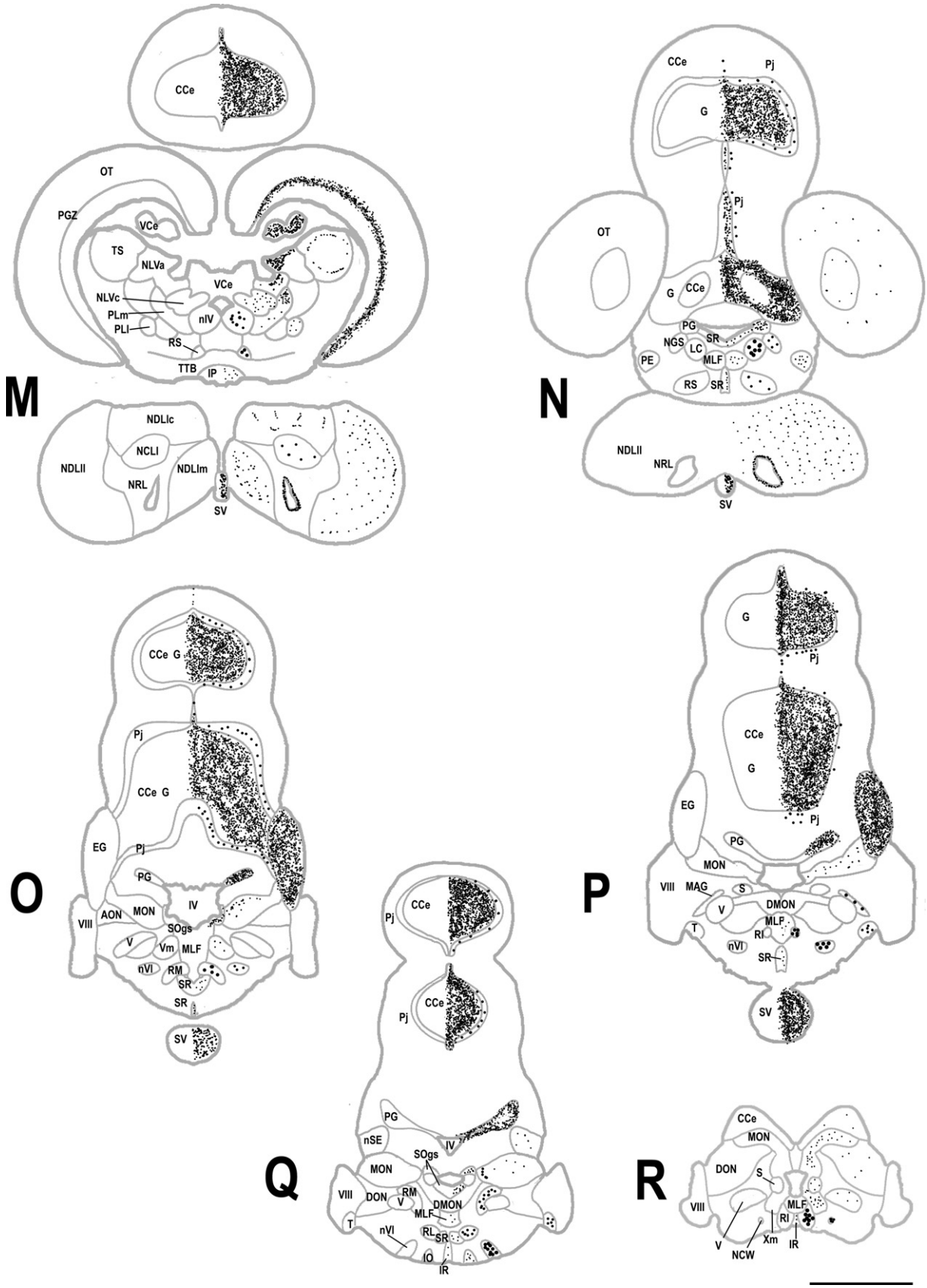

Fig. 4. (*Continued*).

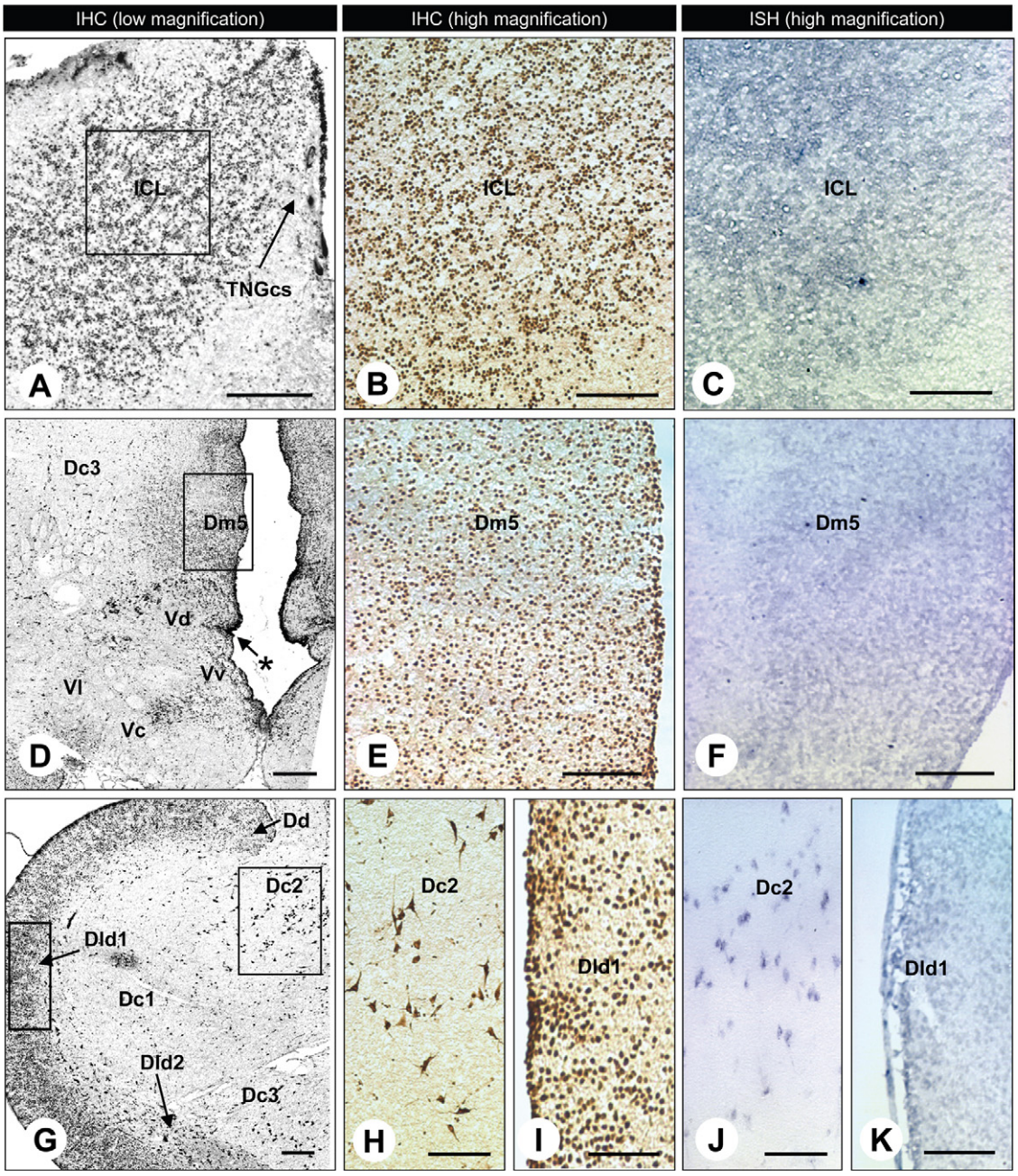

Fig. 5. Distribution of AVT V1a receptor protein in the olfactory bulb and telencephalon showing high concordance with mRNA expression. Low magnification photomicrographs of rock hind brain sections showing AVT V1a receptor protein expression with regions of high expression identified. High magnification micrographs showing high concordance of expression between protein and mRNA are shown in the middle and right, respectively. (A–C) olfactory bulb; (D–F) ventral telencephalon; (G–K) dorsal telencephalon. For abbreviations see Table 1. Scale bars = 200 μm for low magnification and 100 μm for high magnification photomicrographs.

preoptic recess (Figs. 4C–E and 6A–C). The parvocellular preoptic nucleus had many small AVTr-expressing cells packed against the third ventricle and fewer small and medium cells scattered laterally (Fig. 4C–E) with high concordance between protein and mRNA expression (Fig. 6A–C). The parvocellular cells of the magnocellular nucleus had densely packed small cells expressing AVTr arranged in rows near the third ventricle (Figs. 4D and 5F) a pattern also seen in mRNA expression. The magnocellular preoptic nucleus had many AVTr-positive, medium sized cells along the margin of the third ventricle (Figs. 4D and 6A). The gigantocellular preoptic nucleus had very few large cells that expressed AVTr protein and mRNA (Figs. 4D and 6A, D). The anterior periventricular nucleus had many AVTr-positive, small cells around the margin of the third ventricle and few small cells scattered laterally (Fig. 4F) that was also confirmed with mRNA expression.

In the hypothalamus, we observed AVTr mRNA and protein expression in very densely packed small cells in the nucleus of the lateral recess, especially around the margin of the recess (Figs. 4H–N and 7G–I). In the ventral and dorsal parts of the lateral tuberal nucleus (NLTd, NLTv, respectively) we observed small cells densely packed around the margin of the third ventricle that were AVTr-positive for protein and mRNA (Figs. 4F–H and 6G–I). Laterally, the NLTl had larger cells that were AVTr positive (Fig. 4F). The nucleus of the posterior recess had a very dense AVTr immunoreaction (Figs. 4I–K, 7G and 8D), the specificity of which was confirmed with

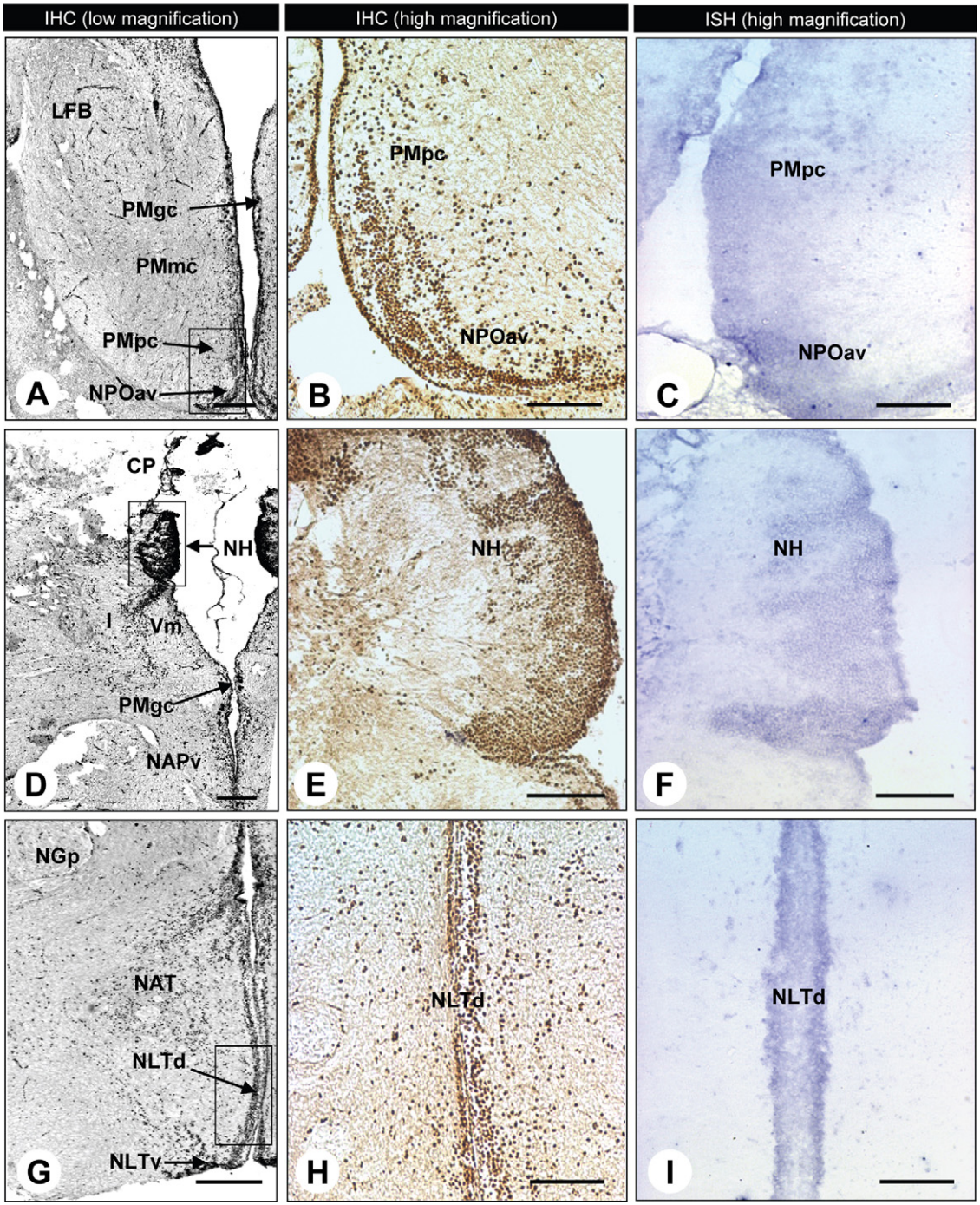

Fig. 6. Distribution of AVT V1a receptor protein in the preoptic area, habenular and lateral tubular nuclei showing high concordance with mRNA expression. Low magnification photomicrographs of rock hind brain sections showing AVT V1a receptor protein expression with regions of high expression identified. High magnification micrographs showing high concordance of expression between protein and mRNA are shown in the middle and right, respectively. (A–C) preoptic nuclei; (D–F) habenular nuclei; (G–I) lateral tubular nuclei. For abbreviations see Table 1. Scale bars = 200 μm for low magnification and 100 μm for high magnification photomicrographs.

mRNA expression in the same region. The nuclei of the saccus vasculosus (NSV; Fig. 4K) and the saccus vasculosus (SV) were both heavily stained for AVTr mRNA and protein (Figs. 4L–P and 8D) as seen in coronet cells that lined the inner recess of the NSV and the outer folds of the SV.

We observed AVTr protein and mRNA expression in several cell types within the inferior lobe of the hypothalamus. The central nucleus of the inferior lobe (Fig. 4M) had expression in many medium sized cells, whereas the lateral part of the diffuse nucleus of the inferior lobe (Fig. 4H–M) and the medial part of the diffuse nucleus of the inferior lobe (Fig. 4M) had expression in many small round and fusiform cells.

3.7. Posterior tuberculum

The periventricular nucleus of the posterior tuberculum (Figs. 4I, J and 7A) and the paraventricular organ (Figs. 4H and 7A) had AVTr protein and mRNA expression in densely packed small cells, particularly near the ventricular wall. AVTr protein expression was observed in small cells and mRNA expression was

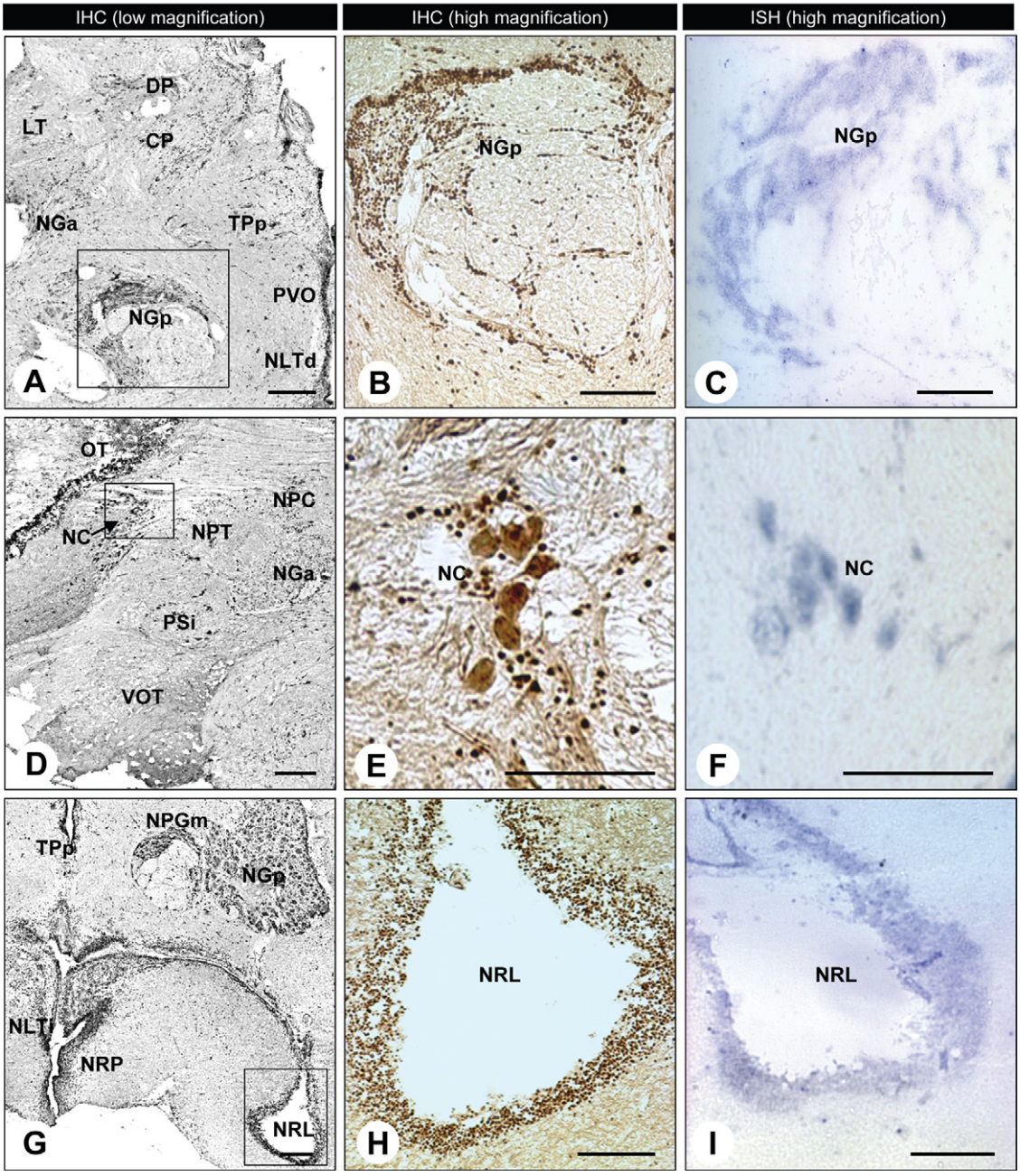

Fig. 7. Distribution of AVT V1a receptor protein in the pretectum, optic tectum and nucleus corticalis; and nuclei of lateral and posterior recesses showing high concordance with mRNA expression. Low magnification photomicrographs of rock hind brain sections showing AVT V1a receptor protein expression with regions of high expression identified. High magnification micrographs showing high concordance of expression between protein and mRNA are shown in the middle and right, respectively. (A–C) pretectum; (D–F) optic tectum and nucleus corticalis; (G–I) nuclei of the lateral and posterior recesses. For abbreviations see Table 1. Scale bars = 200 μm for low magnification and 100 μm for high magnification photomicrographs.

observed in all regions of the preglomerular nucleus: many scattered cells in the prethalamic nucleus (Fig. 4G) and lateral preglomerular nucleus (Fig. 4G); densely packed cells dorsally in the medial preglomerular nucleus (Figs. 4I, J and 5K); and a large area of small, and dense AVTr-expressing cells in the commissural preglomerular nucleus (Figs. 4K, L and 5M). The anterior nucleus glomerulosus (Figs. 4H–K and 7A) had many scattered small round and fusiform cells expressing AVTr protein and mRNA. The posterior nucleus glomerulosus (Figs. 4H–K and 7A, G) had AVTr protein and mRNA expression in small cells surrounding the large glomeruli of this nucleus (Fig. 7B and C, respectively). The tertiary gustatory nucleus had many small cells expressing AVTr (Fig. 4H). The corpus mamillare had very dense AVTr-positive cells in clusters around the margin of the lobes (Figs. 4K, L and 8D, E) that was also seen in mRNA expression (Fig. 8F). The torus lateralis (Fig. 4H–L) had many small and a few medium cells expressing AVTr protein and mRNA, while the lateral thalamic nucleus (Figs. 4I, K and 7A) had a few scattered medium sized cells that were AVTr-positive.

3.8. Thalamus and epithalamus

In the ventral thalamus, the ventromedial thalamic nucleus had many small round cells expressing AVTr at the margin of

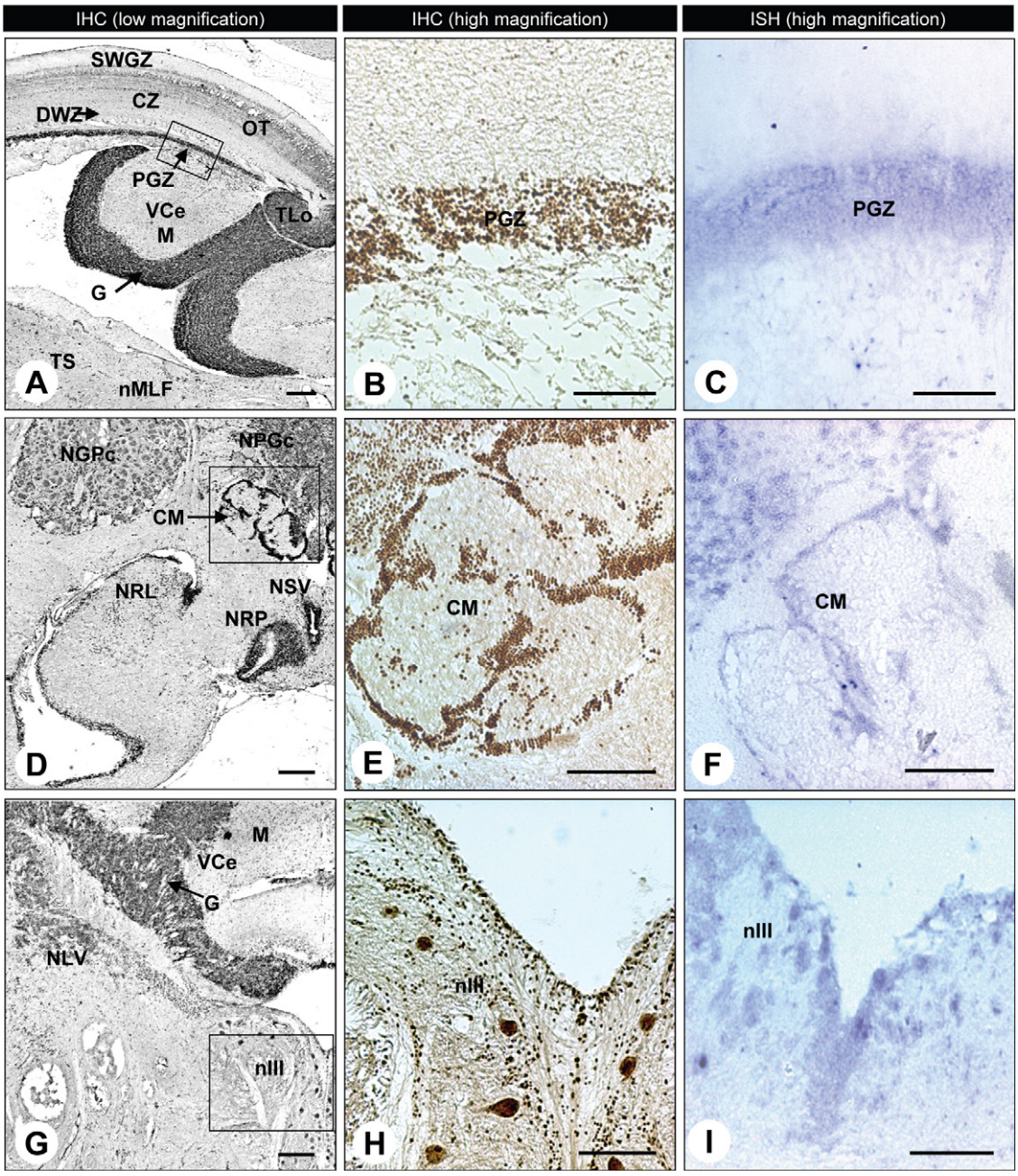

Fig. 8. Distribution of AVT V1a receptor protein in the optic tectum, valvula of the cerebellum (VCe) and torus semicircularis (TS); corpus mamillare (CM) and commissural preglomerular nucleus (NPGc); layers of VCe, and nucleus of the oculomotor nerve (nIII) showing high concordance with mRNA expression. Low magnification photomicrographs of rock hind brain sections showing AVT V1a receptor protein expression with regions of high expression identified. High magnification micrographs showing high concordance of expression between protein and mRNA are shown in the middle and right, respectively. (A–C) zones of optic tectum, valvula of the cerebellum (VCe) and torus semicircularis (TS); (D–F) corpus mamillare (CM) and commissural preglomerular nucleus (NPGc); (G–I) layers of VCe, and nucleus of the oculomotor nerve (nIII). For abbreviations see Table 1. Scale bars = 200 μm for low magnification and 100 μm for high magnification photomicrographs.

the third ventricle and larger fusiform cells scattered laterally (Figs. 4F, G and 6D) which was confirmed in mRNA expression. The intermediate thalamic nucleus had dense, small AVTr-positive cells projecting ventrally from the habenular nucleus expressing both the protein (Figs. 4F and 6D) and mRNA. The dorsal posterior thalamic nucleus (DP) and the central posterior thalamic nucleus (CP) both had many small AVTr-positive cells with protein (Figs. 4G, H and 7A) and mRNA expression.

In the epithalamus, the habenular nucleus was packed with small cells that were AVTr-positive for the protein (Figs. 4F and 6D, E) and mRNA (Fig. 6F). The expression of AVTr protein and mRNA was also observed in the choroid plexus (Fig. 6D).

3.9. Synencephalon

In the pretectum, we observed the highest AVTr protein and mRNA expression in densely packed medium sized cells in the nucleus corticalis (Figs. 4F, G and 7D–F). The dorsal periventricular pretectal nucleus (Fig. 4J) had many small cells that were AVTr-positive for the protein and mRNA. The nucleus of the medial longitudinal fasciculus (Figs. 4H–J and 8A) had large cells that were

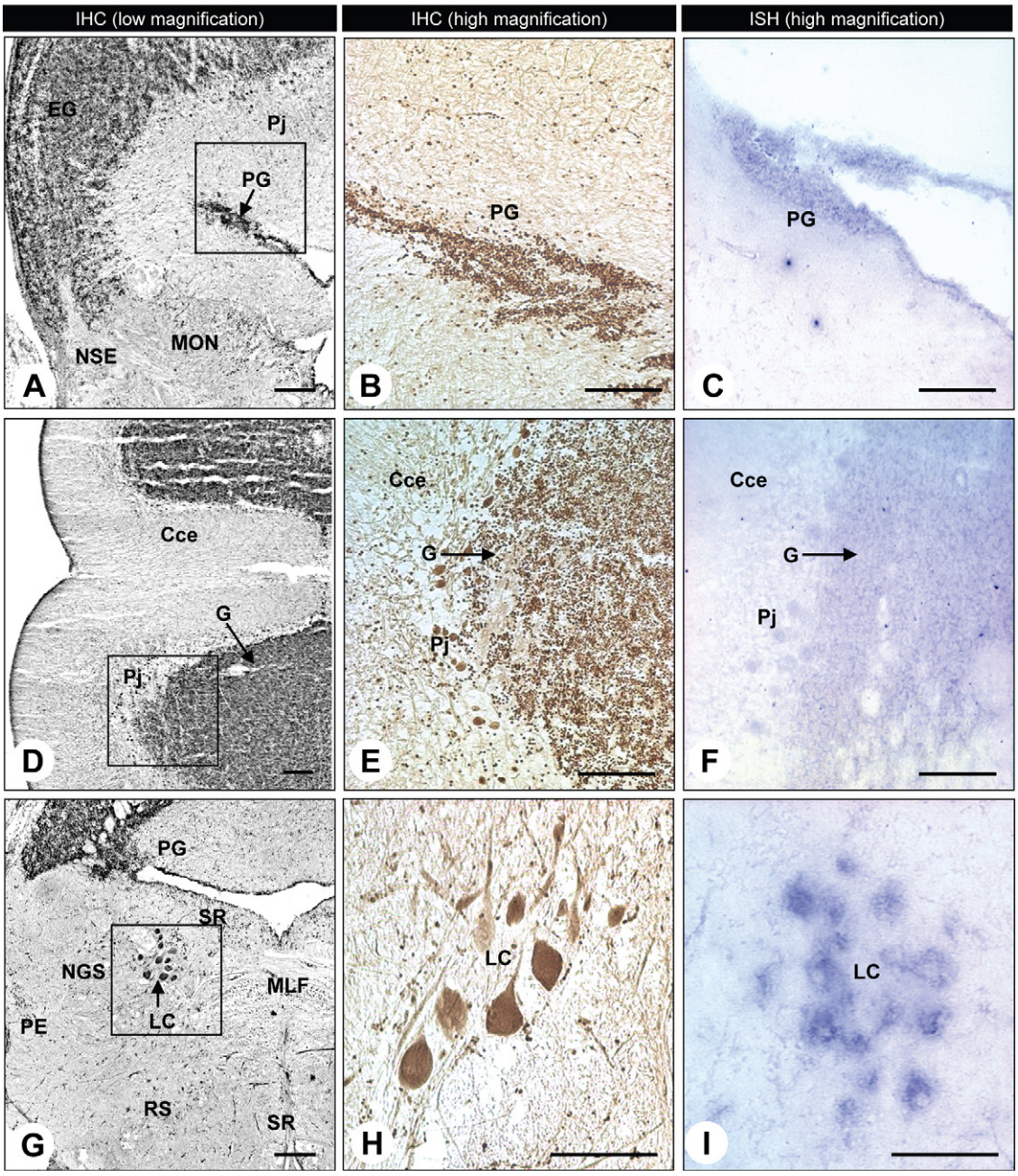

Fig. 9. Distribution of AVT V1a receptor protein in the cerebellar granular eminence (EG) and periventricular granular cell mass of the caudal lobe (PG); corpus cerebelli (CCe) and Purkinje cell layer (Pj); PG and nucleus of the locus coeruleus (LC) showing high concordance with mRNA expression. Low magnification photomicrographs of rock hind brain sections showing AVT V1a receptor protein expression with regions of high expression identified. High magnification micrographs showing high concordance of expression between protein and mRNA are shown in the middle and right, respectively. (A–C) granular eminence (EG) and periventricular granular cell mass of the caudal lobe (PG), (D–F) corpus cerebellum (CCe) and Perkinje cell layer (Pj), (G–I) PG and the locus coeruleus (LC). For abbreviations see Table 1. Scale bars = 200 μm for low magnification and 100 μm for high magnification photomicrographs.

also positive for AVTr protein and mRNA. We observed expression in the accessory pretectal nucleus with many small AVTr-positive cells in a ventromedial orientation (Fig. 4G) that was also confirmed in mRNA expression. The central pretectal nucleus (Figs. 4F, G and 7D) and the nucleus pretectalis (Figs. 4F, G and 7D) had only scattered small cells expressing AVTr. The intermediate superficial pretectal nucleus (Figs. 4G and 7D) had medium cells expressing AVTr around the margin of the round glomerular neuropil, a pattern also seen in mRNA expression. The accessory pretectal nucleus (Fig. 4G) had a narrow margin of small dense cells expressing AVTr protein and mRNA adjacent to DP and CP. We observed only few scattered fusiform and round cells in the dorsal and ventral accessory optic nuclei (Fig. 4G).

3.10. Mesencephalon

In the optic tectum (Fig. 4F–N) we identified four distinct zones pictured in Fig. 8A. Very little AVTr protein expression was seen in the central zone of the optic tectum and in nerve fibers of the deep white zone of the optic tectum. This low level of protein expression was consistent with low mRNA expression. We observed the highest AVTr protein and mRNA expression in small dense cells within the periventricular gray zone (PGZ) (Fig. 8A–C). In the anterior portion of the optic tectum, we also observed small cells lining the periventricular region that were AVTr-positive (Fig. 4F). No AVTr protein or mRNA expression was seen in the superficial white and gray zone. Similar to the PGZ, we observed high

expression in the torus longitudinalis consisting of small dense cells (Figs. 4G–L and 8A) consistent with that of the mRNA expression.

In the mesencephalic tegmentum, high AVTr protein expression was seen in small densely packed cells in the lateral nucleus of the valvula (Figs. 4L, M and 8D) that was confirmed with mRNA expression. Below the fourth ventricle, the oculomotor nucleus had many medium sized fusiform cells expressing AVTr protein (Figs. 4L and 5G, H) and mRNA (Fig. 5I). In the central zone of the tegmentum, the lateral and medial parts of the perilemniscular nucleus had many small fusiform cells expressing AVTr protein and mRNA (Fig. 4M).

3.11. Rhombencephalon

In the valvula of the cerebellum (Figs. 4G–M and 8G) and the corpus cerebellum (Figs. 4H–R and 8D), we observed densely packed granular cells expressing AVTr protein and mRNA (Fig. 8E and F, respectively). Purkinje cells within the CCe (Figs. 4N–Q and 8D) also were AVTr-positive for both protein and mRNA (Fig. 8E and F, respectively). Within the cerebellar vestibulolateral lobe, the granular eminence (Figs. 4O, P and 9A) and the periventricular granular cell mass of the cerebellar caudal lobe (Figs. 4N–Q and 9A) had densely packed small cells expressing AVTr protein and mRNA (Fig. 9B and C, respectively).

In the reticular formation, the superior raphe nucleus had many small cells expressing AVTr protein (Figs. 4N–Q and 9G) and mRNA, whereas the inferior raphe nucleus had fewer small and medium cells expressing AVTr protein (Fig. 4Q–R) and mRNA. The superior reticular nucleus had few medium and large cells expressing AVTr protein (Figs. 4M, N and 9G) and mRNA. The medial reticular nucleus (Fig. 4O–Q) and caudally, the inferior reticular nucleus (Fig. 4P–R) had medium and large cells expressing AVTr, whereas the lateral reticular nucleus was only populated by medium cells that were AVTr-positive (Fig. 4Q).

In the area octavolateralis, the magnocellular octaval nucleus had a thin lamina of large fusiform cells expressing AVTr protein (Fig. 4P) and mRNA. In the tangential nucleus we observed a small cluster of medium sized cells that were AVTr-positive (Fig. 4P–Q). The medial octavolateral nucleus had only few small and medium cells expressing AVTr (Figs. 4O–R and 9A), and the descending octaval nucleus had few scattered small cells expressing AVTr (Fig. 4Q and R). The secondary octaval population had small round cells that were AVTr-positive (Fig. 4O and Q).

In the rhombencephalic somatomotor nuclei, many large cells in the abducens nerve nucleus expressed AVTr protein (Fig. 4O–Q) and mRNA. We were unable to differentiate the facial, vagal, and, glossopharyngeal nucleus; therefore, the collective designation facial-vagal visceromotor column (Xm) was used as in Cerdà-Reverter et al. (2008). The highest expression of AVTr protein and mRNA in this brain region was in large motoneurons within nerve bundles of Xm (Fig. 4R).

In the locus coeruleus, we observed many small cells that were AVTr-positive for protein (Figs. 4N and 9G, H) and mRNA (Fig. 9I). The secondary gustatory nucleus had a few medium cells expressing AVTr (Figs. 4N and 9G) and the inferior olive had a group of small cells arranged dorso-medially that were AVTr-positive for protein and mRNA (Fig. 4Q).

3.12. Pituitary gland

In the pituitary, AVTr protein and mRNA expression was observed. Protein expression was observed in the proximal pars distalis (PPD) in the adenohypophysis but not in the neurohypophysis (Fig. 10). Within the PPD, which contains gonadotrophs, somatotrophs and thyrotrophs in all teleosts investigated to date, medium and large cell types, as well as, cell cluster configurations were AVTr-positive.

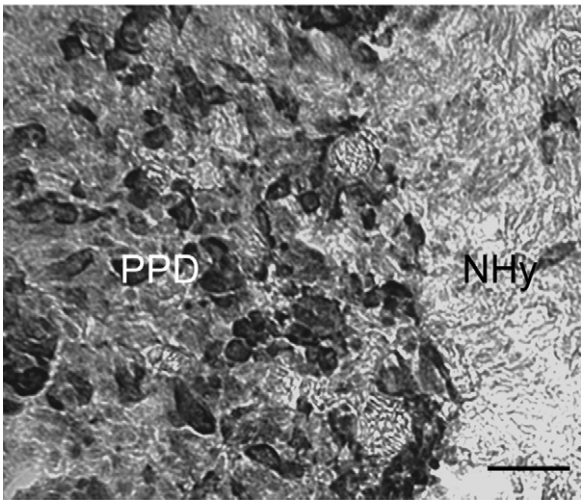

Fig. 10. Distribution of AVT V1a receptor expression in the pituitary of rock hind. Protein expression is seen in large cells of the proximal pars distalis (PPD) in the adenohypophysis but not in the neurohypophysis (NHy). Scale bar = 150 μm.

3.13. Other structures stained for protein and mRNA in rock hind brain

While the main focus of this study was to identify cellular locations of the AVT V1a receptor in rock hind brain, structures other than neuronal cells also expressed AVTr protein and mRNA. Some large blood vessels were stained for protein and mRNA expression however the protein signal was greatly reduced when perfusion techniques were used. In several sections, the meninges were stained for both protein and mRNA expression. Some fiber-rich regions in the optic tectum and valvula of the corpus cerebelli had small structures that were stained for both protein and mRNA.

3.14. Sexual differences

No obvious morphological sex differences were noted in the expression of AVTr protein or mRNA in any region of the rock hind brain. However, these fish were captured outside of the reproductive season and therefore differences between the sexes in reproductively mature fish and/or quantitative differences might exist that were not investigated in this study.

4. Discussion

The present study describes for the first time the distribution of an AVT V1a receptor protein expression throughout the brain of a fish species and verified with its mRNA expression in many of the same regions. The third intracellular loop antigenic site used in this study appears to be specific for the V1a2 receptor subtype. The antigenic sites for the rock hind V1a1 and V1a2 receptors differ substantially (Kline, 2010), as do the V1a1, V1a2 and V2 subtypes identified in pupfish (Lema, 2010). Although a V1b-type vasotocin receptor has yet to be identified in any fish species, the third intracellular loop antigenic site of the three receptor forms differs substantially in newt (Hasunuma et al., 2007). Therefore, the third intracellular loop appears to be an appropriate location for the development of antibodies specific for each vasotocin receptor form identified in rock hind.

The finding of a wide distribution of AVTr protein and mRNA expression in regions throughout the brain of rock hind is

consistent with mRNA distributions of brain microdissections in this (Kline, 2010), as well as in other fish and amphibian species (Hasunuma et al., 2007; Lema, 2010) and in rat (Ostrowski et al., 1994). AVTr was also localized in several areas associated with external sensory processing such as olfaction, vision, and lateral line function (Wullimann, 1998). The expression pattern of the AVT V1a receptor in this study indicates that AVT may act as a neuromodulator via this V1a receptor subtype. AVTr expression in this study was observed in cell bodies as well as in some large blood vessels, meninges and fiber bundles. Large blood vessels, meninges, choroid plexus and white matter structures that did not resemble neurons were also noted to express AVP V1a receptor mRNA in rat brain by Ostrowski et al. (1994). This implies that the site of action for AVT for this receptor is on the membranes of cell bodies and possibly on other neuronal elements.

Although there are few published studies in fish to compare with the present V1a receptor distribution in rock hind, its distribution followed that reported for brain regions in autoradiography experiments with seabass (Moons et al., 1989). In this study, similar expression patterns were seen in the rock hind brain reticular formation as has been reported previously in a study using fluorescently labeled AVT in newt (Lewis et al., 2005). Definitive homology is difficult to determine in many regions of the brain while comparing AVP V1a mapping in the rhesus monkey to the AVT V1a distribution observed in this study. However, several regions that are clearly homologous, namely the inferior olive and locus coeruleus, express AVTr in both species, potentially indicating a conservation of similar functions throughout a wide range of vertebrates. On the other hand, another region with high AVTr expression that appeared similar in the relative position to mammals, the corpus mamillare, has been shown to have highly variable connections and functions even among teleosts (Sawai et al., 2000).

In rock hind brain, AVTr was expressed in regions associated with behavior and reproduction in other vertebrates such as the preoptic region (Foran and Bass, 1999; Goodson and Bass, 2000a; Liu et al., 1997), the tuberal nuclei (Wullimann, 1998) and terminal nerve ganglion cells (TNgc) (Yamamoto et al., 1997). Furthermore, AVTr protein and mRNA were expressed in the parvocellular, magnocellular, and gigantocellular preoptic populations where cells producing AVT and GnRH have been localized in other species (Godwin et al., 2000; Gothilf et al., 1996; Maruska et al., 2007; Mohamed et al., 2005; Senthilkumaran et al., 1999). Although there are no published data on specific cell populations that co-express AVT and GnRH, mRNA expression studies have revealed high expression of both in the POAH of rock hind brain (Kline, 2010). With AVTr expression in this region, there is a potential for feedback on neuropeptide hormone producing neurons such as GnRH and AVT via AVTr within the POAH. High expression of AVTr was also observed in the thalamic nuclei of rock hind brain, the region that has been linked to sexually dimorphic, temporary color patterning and release of gametes in a simultaneous hermaphrodite (Demski and Dulka, 1986).

In rock hind, AVTr expression was observed in the lateral zone of the dorsal telencephalon, subdivision 1 (Dld1) and a previously undescribed region designated subdivision 2 (Dld2). In goldfish, lesions in this area abolish geometric spatial learning in controlled experiments (Vargas et al., 2006). Both male and female rock hind are very territorial and make use of even small visual landmarks to designate territories (Kline et al., 2011). AVT action in these regions could modulate spatial recognition in the males of this very territorial species and should be investigated.

The AVT V1a receptor expression in the adenohypophysis of rock hind pituitary is consistent with that reported in the autoradiography study of seabass (Moons et al., 1989). Although the cell types documented here were not characterized, the effects of AVT have been noted on gonadotropin release in *Poecilia latipinna* (Groves and Batten, 1986) and AVP V1a receptors have been co-localized with follicle stimulating hormone (FSH) and luteinizing hormone (LH) producing cells in rat (Orcel et al., 2002). In newt and pupfish, several AVT receptor subtypes are expressed in the pituitary (Hasunuma et al., 2007; Lema, 2010). The expression of AVT V1a2 receptor in this study in the pituitary cell types warrants further investigation.

Many regions identified for monoamine synthesis had high expression for AVTr protein and mRNA, including the locus coeruleus, a noradrenaline producing region; serotonin producing regions: the raphe nuclei, nucleus of the lateral recess; the dopaminergic periventricular nucleus of the posterior tuberculum (Rink and Wullimann, 2002); and the nucleus of the posterior recess, and posterior periventricular nucleus, which produce both serotonin and dopamine (Fryer et al., 1985; Kah and Chambolle, 1983; Khan and Thomas, 1993);. Thus, AVTr could potentially mediate AVT actions on these monoamine neurotransmitter systems.

AVTr protein and mRNA were highly expressed in the rhombencephalon of rock hind, specifically in the reticular formation and motor control centers that have been linked to the control of sexual behavior such as clasping and response to pheromones in newt (Lewis et al., 2005 and references therein). Hind brain AVTr expression has also been implicated in the control of vocalization in bullfrog, *Rana catesbeiana* (Boyd, 1997). In addition, social approach in goldfish is linked to the medullary areas (Walton et al., 2010) that had high AVT V1a receptor expression in rock hind in this study.

The administration of AVT in fish and amphibians to alter behavior has differing effects in fish with differing reproductive strategies. AVT increases courtship behavior and aggression in the bluehead wrasse (*Thalassoma bifasciatum*) and white perch (*Morone americana*) (Salek et al., 2002; Semsar et al., 2001), and inhibits male specific behavior in damselfish (*Stegastes leucosticctus*) and pupfish (Lema and Nevitt, 2004; Santangelo and Bass, 2006). In the midshipman (*Porichthys notatus*) direct application of AVT to the POA modulates vocalizations (Goodson and Bass, 2000a). In the newt, AVT injections increase male responses to female visual and olfactory stimuli (Thompson and Moore, 2000). Intracerebroventricular injections of AVT have been shown to be more effective at much lower doses in eliciting a response in fish and amphibians (Boyd, 1991; Salek et al., 2002; Santangelo and Bass, 2006), and so it is possible that behavioral effects of AVT could be mediated through a receptor homologous to the V1a receptor reported in this study.

The V1a2 receptor protein and mRNA expression was widespread in the rock hind brain. Although there is no information on the AVT fiber distribution in rock hind, it is widespread in the forebrain of butterflyfish (Dewan et al., 2008) and in the midshipman, AVT innervates many of the regions identified in this study in the preoptic area, hypothalamus, midbrain and hind brain (Goodson and Bass, 2000b). Similarly in frogs (Mathieson, 1996) the VT fibers are present in most brain regions. However it is possible that the AVT system is particularly well developed in the brains of rock hind and other species with a complex social structure. Considering the wide distribution of the AVT V1a2 receptor throughout the brain of rock hind and potentially in other species, behavioral data using large doses of AVP V1a receptor antagonists such as Manning compound should be treated with caution. The antagonists could affect many different pathways within the brain causing the observed behavioral responses.

5. Conclusions

This is the first comprehensive localization of an AVT V1a receptor in a teleost fish. We observed a wide distribution of

receptor protein and mRNA expression throughout brain areas similar to that seen in a study of rat AVP V1a mRNA distribution (Ostrowski et al., 1994). Distinctive regions associated with a wide range of functions were identified, including behavior, reproduction and spatial learning, as well as sensory functions such as vision, olfaction and lateral line sensory processing. Functional and co-localization studies are needed to verify the specific relationship of the V1a receptor to particular cellular functions.

Conflict of interest

No conflicts of interest exist with any of the authors or the data within this manuscript.

Acknowledgements

We acknowledge funding from the Lund Fellowship in Marine Science to RJK and from the Sid Richardson Foundation to GJH and IAK. We also wish to thank Md. Saydur Rahman for helpful comments and assistance with Western blot techniques.

Appendix A. Supplementary data

Supplementary data associated with this article can be found, in the online version, at doi:10.1016/j.jchemneu.2011.06.005.

References

Albers, H.E., Pollock, J., Simmons, W.H., Ferris, C.F., 1986. A V1-like receptor mediates vasopressin-induced flank marking behavior in hamster hypothalamus. J. Neurosci. 6, 2085–2089.
Baeyens, D.A., Cornett, L.E., 2006. The cloned avian neurohypophysial hormone receptors. Comp. Biochem. Phys. B 143, 12–19.
Balment, R.J., Lu, W., Weybourne, E., Warne, J.M., 2006. Arginine vasotocin a key hormone in fish physiology and behaviour: A review with insights from mammalian models. Gen. Comp. Endocr. 147, 9–16.
Birnbaumer, M., 2000. Vasopressin receptors. Trends Endocrinol. Metab. 11, 406–410.
Boyd, S.K., 1991. Effect of vasotocin on locomotor activity in bullfrogs varies with developmental stage and sex. Horm. Behav. 25, 57–69.
Boyd, S.K., 1997. Brain vasotocin pathways and the control of sexual behaviors in the bullfrog. Brain Res. Bull. 44, 345–350.
Cerdà-Reverter, J.M., Muriach, B., Zanuy, S., Muñoz-Cueto, J.A., 2008. A cytoarchitectonic study of the brain of a perciform species, the sea bass (*Dicentrarchus labrax*): the midbrain and hindbrain. Acta Histochem. 110, 433–450.
Cerdà-Reverter, J.M., Zanuy, S., Muñoz-Cueto, J.A., 2001a. Cytoarchitectonic study of the brain of a perciform species, the sea bass (*Dicentrarchus labrax*). I. The telencephalon. J. Morphol. 247, 217–228.
Cerdà-Reverter, J.M., Zanuy, S., Muñoz-Cueto, J.A., 2001b. Cytoarchitectonic study of the brain of a perciform species, the sea bass (*Dicentrarchus labrax*). II. The diencephalon. J. Morphol. 247, 229–251.
Conklin, D.J., Smith, M.P., Olson, K.R., 1999. Pharmacological characterization of arginine vasotocin vascular smooth muscle receptors in the trout (*Oncorhynchus mykiss*) *in vitro*. Gen. Comp. Endocrinol. 114, 36–46.
Demski, L.S., Dulka, J.G., 1986. Thalamic stimulation evokes sex–color change and gamete release in a vertebrate hermaphrodite. Experientia 42, 1285–1287.
Dewan, A.K., Maruska, K.P., Tricas, T.C., 2008. Arginine vasotocin neuronal phenotypes among congeneric territorial and shoaling reef butterflyfishes: species, sex and reproductive season comparisons. J. Neuroendocrinol. 20, 1382–1394.
Foran, C.M., Bass, A.H., 1999. Preoptic GnRH and AVT: axes for sexual plasticity in teleost fish. Gen. Comp. Endocrinol. 116, 141–152.
Fryer, J.N., Boudreault-Chateauvert, C., Kirby, R.P., 1985. Pituitary afferents originating in the paraventricular organ (PVO) of the goldfish hypothalamus. J. Comp. Neurol. 242, 475–484.
Godwin, J., Sawby, R., Warner, R.R., Crews, D., Grober, M.S., 2000. Hypothalamic arginine vasotocin mRNA abundance variation across sexes and with sex change in a coral reef fish. Brain Behav. Evol. 55, 77–84.
Goodson, J.L., Bass, A.H., 2000a. Forebrain peptides modulate sexually polymorphic vocal circuitry. Nature 403, 769–772.
Goodson, J.L., Bass, A.H., 2000b. Vasotocin innervation and modulation of vocal-acoustic circuitry in the teleost *Porichthys notatus*. J. Comp. Neurol. 422, 363–379.
Gothilf, Y., Munoz-Cueto, J.A., Sagrillo, C.A., Selmanoff, M., Chen, T.T., Kah, O., Elizur, A., Zohar, Y., 1996. Three forms of gonadotropin-releasing hormone in a perciform fish (*Sparus aurata*): complementary deoxyribonucleic acid characterization and brain localization. Biol. Reprod. 55, 636–645.
Grober, M.S., Sunobe, T., 1996. Serial adult sex change involves rapid and reversible changes in forebrain neurochemistry. Neuroreport 7, 2945–2949.
Groves, D.J., Batten, T.F.C., 1986. Direct control of the gonadotroph in a teleost *Poecilia latipinna*. II. Neurohormones and neurotransmitters. Gen. Comp. Endocrinol. 62, 315–326.
Hasunuma, I., Sakai, T., Nakada, T., Toyoda, F., Namiki, H., Kikuyama, S., 2007. Molecular cloning of three types of arginine vasotocin receptor in the newt, *Cynops pyrrhogaster*. Gen. Comp. Endocrinol. 151, 252–258.
Hayashi, M., Sasaki, S., Tsuganezawa, H., Monkawa, T., Kitajima, W., Konishi, K., Fushimi, K., Marumo, F., Saruta, T., 1994. Expression and distribution of aquaporin of collecting duct are regulated by vasopressin V-2 receptor in rat kidney. J. Clin. Invest. 94, 1778–1783.
Insel, T.R., Wang, Z.X., Ferris, C.F., 1994. Patterns of brain vasopressin receptor distribution associated with social-organization in microtine rodents. J. Neurosci. 14, 5381–5392.
Iwata, E., Nagai, Y., Sasaki, H., 2008. Social rank modulates brain arginine vasotocin immunoreactivity in false clown anemonefish (*Amphiprion ocellaris*). Fish Physiol. Biochem. 36, 337–345.
Jurkevich, A., Berghman, L.R., Cornett, L.E., Kuenzel, W.J., 2005. Characterization and immunohistochemical visualization of the vasotocin VT2 receptor in the pituitary gland of the chicken, *Gallus gallus*. Gen. Comp. Endocrinol. 143, 82–91.
Kah, O., Chambolle, P., 1983. Serotonin in the brain of the goldfish *Carassius auratus*. An immunocytochemical study. Cell Tissue Res. 234, 319–333.
Khan, I.A., Thomas, P., 1993. Immunocytochemical localization of serotonin and gonadotropin-releasing-hormone in the brain and pituitary gland of the Atlantic croaker *Micropogonias undulatus*. Gen. Comp. Endocrinol. 91, 167–180.
Kline, R.J., 2010. Hormonal correlates of coloration and sexual change in the hermaphroditic grouper, *Epinephelus adscensionis*. Ph.D. Thesis, The University of Texas at Austin.
Kline, R.J., Khan, I.A., Holt, G.J., 2011. Behavior, color change and time for sexual inversion in the protogynous grouper (*Epinephelus adscensionis*). PLoS ONE 6, e19576.
Lema, S.C., 2010. Identification of multiple vasotocin receptor cDNAs in teleost fish: sequences, phylogenetic analysis, sites of expression, and regulation in the hypothalamus and gill in response to hyperosmotic challenge. Mol. Cell. Endocrinol. 321, 215–230.
Lema, S.C., Nevitt, G.A., 2004. Exogenous vasotocin alters aggression during agonistic exchanges in male Amargosa River pupfish (*Cyprinodon nevadensis amargosae*). Horm. Behav. 46, 628–637.
Lewis, C.M., Dolence, E.K., Hubbard, C.S., Rose, J.D., 2005. Identification of roughskin newt medullary vasotocin target neurons with a fluorescent vasotocin conjugate. J. Comp. Neurol. 491, 381–389.
Liu, Y.C., Salamone, J.D., Sachs, B.D., 1997. Lesions in medial preoptic area and bed nucleus of stria terminalis: differential effects on copulatory behavior and noncontact erection in male rats. J. Neurosci. 17, 5245–5253.
Mahlmann, S., Meyerhof, W., Hausmann, H., Heierhorst, J., Schonrock, C., Zwiers, H., Lederis, K., Richter, D., 1994. Structure, function, and phylogeny of [Arg(8)] vasotocin receptors from Teleost fish and toad. Proc. Natl. Acad. Sci. U. S. A. 91, 1342–1345.
Manning, M., Sawyer, W.H., 1993. Design, synthesis and some uses of receptor-specific agonists and antagonists of vasopressin and oxytocin. J. Receptor Res. 13, 195–214.
Maruska, K.P., Mizobe, M.H., Tricas, T.C., 2007. Sex and seasonal co-variation of arginine vasotocin (AVT) and gonadotropin-releasing hormone (GnRH) neurons in the brain of the halfspotted goby. Comp. Biochem. Phys. A 147, 129–144.
Mathieson, W.B., 1996. Development of arginine vasotocin innervation in two species of anuran amphibian: *Rana catesbeiana* and *Rana sylvatica*. Histochem. Cell Biol. 105, 305–318.
Mohamed, J.S., Thomas, P., Khan, I.A., 2005. Isolation, cloning, three prepro-GnRH and expression of mRNAs in Atlantic croaker brain and pituitary. J. Comp. Neurol. 488, 384–395.
Moons, L., Cambre, M., Batten, T.F.C., Vandesande, F., 1989. Autoradiographic localization of binding-sites for vasotocin in the brain and pituitary of the sea bass (*Dicentrarchus labrax*). Neurosci. Lett. 100, 11–16.
Moore, F.L., Miller, L.J., 1983. Arginine vasotocin induces sexual behavior of newts by acting on cells in the brain. Peptides 4, 97–102.
Munchrath, L.A., Hofmann, H.A., 2010. Distribution of sex steroid hormone receptors in the brain of an African cichlid fish, *Astatotilapia burtoni*. J. Comp. Neurol. 518, 3302–3326.
Nair, H.P., Young, L.J., 2006. Vasopressin and pair-bond formation: genes to brain to behavior. Physiology (Bethesda) 21, 146–152.
Northcutt, R.G., Davis, R.E., 1983. Telencephalic organization in ray-finned fishes. In: Davis, R.E., Northcutt, R.G. (Eds.), Fish Neurobiology. University of Michigan Press, Ann Arbor, pp. 203–236.
Orcel, H., Tobin, V.A., Alonso, G., Rabie, A., 2002. Immunocytochemical localization of vasopressin V1a receptors in the rat pituitary gonadotropes. Endocrinology 143, 4385–4388.
Ostrowski, N.L., Lolait, S.J., Young, W.S., 1994. Cellular localization of vasopressin V1a receptor messenger-ribonucleic-acid in adult male rat brain, pineal, and brain vasculature. Endocrinology 135, 1511–1528.
Rink, E., Wullimann, M.F., 2002. Connections of the ventral telencephalon and tyrosine hydroxylase distribution in the zebrafish brain (*Danio rerio*) lead to

identification of an ascending dopaminergic system in a teleost. Brain Res. Bull. 57, 385–387.
Salek, S.J., Sullivan, C.V., Godwin, J., 2002. Arginine vasotocin effects on courtship behavior in male white perch (*Morone americana*). Behav. Brain Res. 133, 177–183.
Santangelo, N., Bass, A.H., 2006. New insights into neuropeptide modulation of aggression: field studies of arginine vasotocin in a territorial tropical damselfish. Proc. R. Soc. B 273, 3085–3092.
Sawai, N., Yamamoto, N., Yoshimoto, M., Ito, H., 2000. Fiber connections of the corpus mamillare in a percomorph teleost, tilapia *Oreochromis niloticus*. Brain Behav. Evol. 55, 1–13.
Semsar, K., Kandel, F.L.M., Godwin, J., 2001. Manipulations of the AVT system shift social status and related courtship and aggressive behavior in the bluehead wrasse. Horm. Behav. 40, 21–31.
Senthilkumaran, B., Okuzawa, K., Gen, K., Ookura, T., Kagawa, H., 1999. Distribution and seasonal variations in levels of three native GnRHs in the brain and pituitary of Perciform fish. J. Neuroendocrinol. 11, 181–186.
Serradeil-Le Gal, C., Wagnon, J., Valette, G., Garcia, G., Pascal, M., Maffrand, J.P., Le Fur, G., 2002. Nonpeptide vasopressin receptor antagonists: development of selective and orally active V1a, V2 and V1b receptor ligands. Prog. Brain Res. 139, 197–210.
Tanoue, A., Ito, S., Honda, K., Oshikawa, S., Kitagawa, Y., Koshimizu, T., Mori, T., Tsujimoto, G., 2004. The vasopressin V1b receptor critically regulates hypothalamic–pituitary–adrenal aids activity under both stress and resting conditions. J. Clin. Invest. 113, 302–309.
Thompson, R.R., Moore, F.L., 2000. Vasotocin stimulates appetitive responses to the visual and pheromonal stimuli used by male roughskin newts during courtship. Horm. Behav. 38, 75–85.
Vargas, J.P., Bingman, V.P., Portavella, M., Lopez, J.C., 2006. Telencephalon and geometric space in goldfish. Eur. J. Neurosci. 24, 2870–2878.
Walton, J.C., Waxman, B., Hoffbuhr, K., Kennedy, M., Beth, E., Scangos, J., Thompson, R.R., 2010. Behavioral effects of hindbrain vasotocin in goldfish are seasonally variable but not sexually dimorphic. Neuropharmacology 58, 126–134.
Warne, J.M., 2001. Cloning and characterization of an arginine vasotocin receptor from the euryhaline flounder *Platichthys flesus*. Gen. Comp. Endocrinol. 122, 312–319.
Warne, J.M., Bond, H., Weybourne, E., Sahajpal, V., Lu, W., Balment, R.J., 2005. Altered plasma and pituitary arginine vasotocin and hypothalamic provasotocin expression in flounder (*Platichthys flesus*) following hypertonic challenge and distribution of vasotocin receptors within the kidney. Gen. Comp. Endocrinol. 144, 240–247.
Winslow, J.T., Hastings, N., Carter, C.S., Harbaugh, C.R., Insel, T.R., 1993. A role for central vasopressin in pair bonding in monogamous prairie voles. Nature 365, 545–548.
Wullimann, M.F., 1998. The central nervous system. In: Evans, D.H. (Ed.), The Physiology of Fishes. 2nd ed. CRC Press, Boca Raton, FL, pp. 247–284.
Wullimann, M.F., Rupp, B., Reichert, H., 1996. Neuroanatomy of the Zebrafish Brain: A Topological Atlas. Verlag, Boston.
Yamamoto, N., Oka, Y., Kawashima, S., 1997. Lesions of gonadotropin-releasing hormone-immunoreactive terminal nerve cells: effects on the reproductive behavior of male dwarf gouramis. Neuroendocrinology 65, 403–412.